Eidgenössische Technische Hochschule Zürich

Ecole polytechnique fédérale de Zurich
Politecnico federale di Zurigo
Swiss Federal Institute of Technology Zurich

A numerical study on Neumann-Neumann and FETI methods for *hp*-approximations on geometrically refined boundary layer meshes in two dimensions*

A. Toselli and X. Vasseur

Research Report No. 2002-20
October 2002

Seminar für Angewandte Mathematik
Eidgenössische Technische Hochschule
CH-8092 Zürich
Switzerland

*This work was partially supported by the Swiss National Science Foundation under Project 20-63397.00

A numerical study on Neumann-Neumann and FETI methods for *hp*-approximations on geometrically refined boundary layer meshes in two dimensions*

A. Toselli and X. Vasseur

Seminar für Angewandte Mathematik
Eidgenössische Technische Hochschule
CH-8092 Zürich
Switzerland

Research Report No. 2002-20 October 2002

Abstract

In this paper, we present extensive numerical tests showing the performance and robustness of certain Balancing Neumann-Neumann and one–level FETI methods for the solution of algebraic linear systems arising from *hp* finite element approximations of scalar elliptic problems on geometrically refined boundary layer meshes in two dimensions. The numerical results are in good agreement with the theoretical bounds for the condition numbers of the preconditioned operators derived in [44]. They confirm that the condition numbers are independent of the aspect ratio of the mesh and of potentially large jumps of the coefficients. In addition, they only grow polylogarithmically with the polynomial degree, as in the case of p approximations on shape-regular meshes. Our methods are robust with respect to small parameters of certain singularly-perturbed problems.

Keywords: Domain decomposition, preconditioning, *hp* finite elements, spectral elements, anisotropic meshes

Subject Classification: 65N22, 65N55, 65N35

*This work was partially supported by the Swiss National Science Foundation under Project 20-63397.00

1 Introduction

In order to make the iterative solution of large systems of finite element equations possible and efficient on parallel architectures, domain decomposition (DD) techniques have been used extensively in recent years; see, e.g., the monographs [36, 41]. These methods are by now well-understood in various *standard* situations; cf. [2, 4, 9, 18, 19, 20, 31] and the references therein for some work on *hp* approximations. However many problems in engineering practice are "less-standard" at least for three reasons. First, the required meshes may be highly anisotropic. This feature is known to be essential to ensure optimal resolution of boundary layers in fluid dynamics for instance. Secondly, the computational domains may be highly irregular and complex (see, e.g., [42] where various industrial applications in computational fluid dynamics and computational mechanics are described) or extremely thin (such as plates, shells, and thin films). Finally the equations may be singularly-perturbed due to the presence of small parameters, as in, e.g., convection dominated flows or shells.

In the worst case, the possible combination of these factors can lead to prohibitively large condition numbers for the stiffness matrix and efficient iterative solvers are thus needed. Many crucial issues still need to be addressed and solved in order to obtain robust iterative solvers on highly anisotropic meshes and very thin domains for both regular and singularly-perturbed problems; see, e.g., [24, 26] for some work for p-finite elements on thin domains. The goal of this and of our previous paper [44] is to present a first preliminary analysis and numerical study on some domain decomposition methods of iterative substructuring type.

Balancing Neumann-Neumann [25] and one-level Finite Element Tearing and Interconnecting (FETI) [16] methods are considered in this work. They rely on a non-overlapping partition into subdomains (substructures). They are among the most popular domain decomposition methods for the iterative solution of algebraic systems arising from the finite element approximation of elliptic partial differential equations and present certain advantages over other iterative substructuring methods, like, for instance, the fact that the subdomain partition does not need to be a coarse mesh but very general substructures can be considered, and that they can equivalently be employed for two and three dimensional problems. In addition, they share many algorithmic components such as suitable scaling matrices built with the coefficients of the partial differential equation, local solvers for both Neumann and Dirichlet problems on the substructures, and the use of a coarse space to ensure scalability where basis coarse functions are associated to the single substructures. Both methods lead to positive definite preconditioned operators on appropriate subspaces allowing the use of Conjugate Gradient as an iterative solver [7]. A recent theoretical study has been developed in [44], where the authors proposed some efficient iterative substructuring methods for *hp* finite element approximations on two-dimensional geometrically refined meshes. The main focus in [44] is robustness

with respect to arbitrarily high aspect ratio of the mesh. The main theoretical result of that work is that certain Balancing Neumann-Neumann and one-level FETI methods provide condition numbers independent of the aspect ratio of the mesh and of potentially large jumps of the coefficients, still retaining a polylogarithmic growth in the number of unknowns. This theoretical analysis has been developed on a simple diffusion problem and few numerical experiments on a singularly-perturbed reaction-diffusion problem have also been provided. Both preconditioners have been found to be robust with respect to the perturbation parameter and the aspect ratio of the mesh. The goal of this paper is to provide an extensive numerical study to show that the theoretical bounds proven in [44] also appear to hold for different and more complicated elliptic problems possibly of singularly-perturbed type.

The remainder of this paper is organized as follows: in section 2, we introduce the model problem for our proposed numerical study. In sections 3 and 4, *hp* finite element approximations and a class of geometrically refined meshes, respectively, are introduced. Our domain decomposition preconditioners are described in section 5. In section 6 we present some bounds on the condition number of certain unpreconditioned and preconditioned operators, while an extensive numerical study is presented in section 7. We end this work by mentioning some perspectives and future developments in section 8.

2 Problem setting

In this paper, we consider the following linear elliptic problem on a bounded polygonal domain $\Omega \subset \mathbb{R}^2$:

$$\begin{aligned} &-\varepsilon_x \frac{\partial}{\partial x}(\rho_x \frac{\partial u}{\partial x}) - \varepsilon_y \frac{\partial}{\partial y}(\rho_y \frac{\partial u}{\partial y}) + c\, u = f, \quad \text{in } \Omega, \\ &u = u_D, \qquad\qquad\qquad\qquad\qquad\qquad\quad \text{on } \partial\Omega \end{aligned} \tag{1}$$

where (ρ_x, ρ_y) are real and positive diffusion coefficients, $(\varepsilon_x, \varepsilon_y)$ are real and positive, possibly small, constants and c is a non-negative reaction coefficient. Throughout this paper we refer to this problem as Problem (M). We note that, if $c > 0$ and the source term f is not compatible with the boundary datum u_D, Problem (M) does not admit a solution for $\varepsilon_x = 0$ or $\varepsilon_y = 0$ and a boundary layer of width $\sqrt{\varepsilon_x}$ or $\sqrt{\varepsilon_y}$ is present along $\partial\Omega$ for small values of the parameters. Thus highly refined meshes near $\partial\Omega$ are needed to ensure robust exponential convergence of the approximate solution; see, e.g., [30, 39, 40].

In our work, Ω is chosen as the unit square $(0,1)^2$, although the theoretical analysis provided in [44] is valid for more general polygonal domains. For simplicity, we only consider Dirichlet boundary conditions, but more general Neumann or mixed boundary conditions can also be used. The constants $(\varepsilon_x, \varepsilon_y)$ can be arbitrarily small in some problems and this leads to a class of singularly-perturbed problems. The coefficients (ρ_x, ρ_y) can be discontinuous, with very

different values for different subregions of Ω. Finally the scalar function c may arise from a finite difference discretization of a time derivative for example. We also note that purely diffusive problems correspond to the case $c = 0$.

Remark 2.1 *Problem (M) is only a model problem for certain diffusion-reaction phenomena. Convection-dominated problems are another important class of problems that may require highly stretched meshes and thus can be relevant to test the performances of our domain decomposition preconditioners. Nevertheless this study is left to a future work. We note however that the Robin-Robin and FETI methods developed for scalar advection-diffusion problems in [1] and [43], respectively, can be employed.*

3 *hp* finite element approximations

Given an affine quadrilateral mesh $\mathcal{T}$ of Ω and a polynomial degree $k \geq 1$, we consider the following finite element space

$$X^k(\Omega;\mathcal{T}) = \left\{u \in H^1(\Omega) \,|\quad u_{|_K} \in \mathbb{Q}_k(K),\ K \in \mathcal{T}\right\}. \tag{2}$$

Here $H^1(\Omega)$ is the space of square summable functions with square summable first derivatives and $\mathbb{Q}_k(K)$ is the space of polynomials of maximum degree k in each variable on K. In this paper, interpolating Lagrange polynomials on Gauss-Lobatto nodes are used as a particular nodal basis of $X^k(\Omega;\mathcal{T})$. We recall that the set of Gauss-Lobatto points $GLL(k)$ is the set of (distinct and real) zeros of $(1-x^2)L'_{k-1}(x)$, with L_{k-1} the Legendre polynomial of degree $k-1$ (cf. [8, Sect. 3]) and that the quadrature formula based on $GLL(k)$ has order $2k-1$. Exact numerical integration is adopted in this work. Thus quadrature formulas based either on $GLL(k)$ for purely diffusive problems or $GLL(k+1)$ for reaction-diffusion problems are chosen. Given the nodes $GLL(k)^2$ on the reference element $\hat{Q} = (-1,1)^2$, our basis functions on $\mathbb{Q}_k(\hat{Q})$ are defined as the tensor product of k-th order Lagrange interpolating polynomials on $GLL(k)$. More details on spectral element methods can be found in, e.g., [8] for instance.

Irregular meshes can be employed for conforming *hp* finite element approximations. We recall that the mesh $\mathcal{T}$ is said to be *regular* if the intersection between neighboring elements is either a vertex or an entire edge of both elements. We only consider regular meshes in this work. Indeed, we cannot treat irregular meshes with hanging nodes yet. This restriction, explained in [44] in more details, is due to the difficulty in the construction of iterative substructuring methods in presence of hanging nodes, especially when they lie on the interface between subdomains. Presently, we are unaware of any domain decomposition method of iterative substructuring type that can be applied to approximations on irregular meshes and that leads to the same condition number bounds (17) and (23). This issue is left to a future work and seems to be crucial, especially for three-dimensional applications; see also Section 4 for additional comments.

The spectral polynomial degree k is also assumed to be the same on all the elements in our experiments.

4 Geometric boundary layer meshes

In order to resolve boundary layers and/or singularities, geometrically graded meshes can be employed. They are determined by a mesh grading factor $\sigma \in (0,1)$ and by the refinement level n. The number of layers is $n+1$ and the thinnest layer has a width proportional to σ^n. With an abuse of notation, we refer to n as the number of layers in the following. Robust exponential convergence of hp finite element approximations is achieved if n is suitably chosen. For singularity resolution, n is required to be proportional to the polynomial degree k; see [3, 5]. In the presence of boundary layers, the width of the thinnest layer needs to be comparable to that of the boundary layer; see [30, 39, 40]. In practical applications, for boundary layers of fixed width, and corner (and edge, in three dimensions) singularities, n is usually chosen proportional to the polynomial degree k, with the assumption that k is sufficiently large.

A two-dimensional geometric boundary layer mesh $\mathcal{T} = \mathcal{T}_{bl}^{n,\sigma}$ is, roughly speaking, the tensor product of meshes that are geometrically refined towards the edges; see Figures 4 and 6 for two examples of meshes refined towards two edges.

The mesh $\mathcal{T}$ is built by first considering an initial, shape-regular macro-triangulation $\mathcal{T}^0$ which is successively refined. Every macroelement can be refined isotropically or anisotropically in order to obtain edge or corner patches. Here, we only describe patches obtained by triangulating the reference square $\hat{Q} := I^2$, with $I := (-1,1)$. A patch for an element $K^0 \in \mathcal{T}^0$ is obtained by using an affine mapping $F_{K^0} : \hat{Q} \to K^0$.

Edge and **corner patches** are given by anisotropic triangulations of the form

$$\mathcal{T}_e := \{I \times K_y \mid \quad K_y \in \mathcal{T}_y\}, \qquad \mathcal{T}_c := \{K_x \times K_y \mid \quad K_x \in \mathcal{T}_x,\ K_y \in \mathcal{T}_y\},$$

respectively, where $\mathcal{T}_x$ and $\mathcal{T}_y$ are meshes of I, geometrically refined towards one vertex (say -1), with grading factor $\sigma \in (0,1)$ and n layers; see Figure 6, for a mesh with $\sigma = 0.5$ and $n = 6$. More precisely, $\mathcal{T}_x$ and $\mathcal{T}_y$ are built recursively, by subdividing the element that contains the vertex -1 into two smaller intervals in a $\sigma : (1-\sigma)$ ratio.

The number of degrees of freedom associated to one single element is $O(k^2)$. The number of elements in an edge and corner patch with n layers is $O(n)$ and $O(n^2)$, respectively. Consequently, if $n = O(k)$, as is required for exponential convergence, the corresponding FE spaces have $O(k^3)$ and $O(k^4)$ degrees of freedom, respectively.

A geometric boundary layer mesh $\mathcal{T}$ satisfies the following properties:

Property 4.1 *$\mathcal{T}$ is obtained from an initial shape-regular coarse mesh $\mathcal{T}^0$ (macromesh) by local isotropic or anisotropic refinement.*

Property 4.2 *Anisotropic refinement is always performed towards the boundary $\partial\Omega$ of the computational domain Ω and never towards the interior.*

Figures 4 and 6 highlight these features. Both properties appear so far to be essential to derive efficient iterative substructuring methods; see section 6 and [44] for more details.

We note that boundary layer meshes are regular and can also be employed in polygonal domains when no boundary layers, but only singularities are present. However, only refinement towards corners is necessary in this case. This can be done more efficiently by considering coarser irregular meshes, geometrically refined only towards corners, which still provide the same accuracy with fewer elements; see, e.g., Figure 2 in [44]. In this case, a corner patch has indeed $O(n)$ elements and thus only $O(k^3)$ degrees of freedom.

5 Iterative substructuring methods

Given a geometric boundary layer mesh $\mathcal{T}$ and a spectral polynomial degree k, a function $u \in X^k(\Omega;\mathcal{T})$ is expanded using the basis functions described in section 3. The finite element approximation of Problem (M) thus leads to a linear system

$$A\,u = b\,,$$

with A symmetric, positive-definite. The condition number of A can be huge for large values of k and n (see section 6) and efficient and robust preconditioners are therefore often mandatory. We investigate Balancing Neumann-Neumann ([25]) and one-level FETI ([16]) iterative methods. A presentation is given in sections 5.2 and 5.3. The theoretical bounds for the condition numbers are presented in sections 5.2.3 and 5.3.3 respectively without proof. We refer the reader to [44] for their derivation. More general information on domain decomposition methods can be found in the monographs [36, 41].

5.1 Subdomain partitions

Iterative substructuring methods rely on a non-overlapping partition of Ω, $\mathcal{T}^{DD} = \{\Omega_i\}$, into substructures. Let N denote the number of substructures with H_i the diameter of Ω_i and $H = \max(H_i)$ the maximum of their diameters. A subdomain Ω_i is called *floating* if the intersection of $\partial\Omega_i$ with $\partial\Omega$ is empty. We define the boundaries $\Gamma_i = \partial\Omega_i \setminus \partial\Omega$ and the interface Γ as their union. The sets of Gauss-Lobatto nodes and the corresponding degrees of freedom on $\partial\Omega_i$, Γ, and $\partial\Omega$ are denoted by $\partial\Omega_{i,h}$, Γ_h, and $\partial\Omega_h$, respectively.

In this work, the main geometric assumption on the substructures is that they be *shape-regular*. This property appears to be essential to obtain the

condition number bounds presented in sections 5.2.3 and 5.3.3. Indeed, Property 4.1 allows us to fulfill this condition easily by choosing the macromesh as the subdomain partition:

$$\mathcal{T}^{DD} = \mathcal{T}^0.$$

A consequence of Property 4.2 is then that, when two substructures share an interior vertex, the local meshes are shape-regular in the neighborhood of this vertex, since anisotropic refinement is only performed towards the boundary $\partial\Omega$. This property also appears to be essential to obtain the condition number bounds in sections 5.2.3 and 5.3.3.

5.2 Balancing Neumann-Neumann methods

5.2.1 Derivation

After subassembling, the stiffness matrix A is reordered according to the domain decomposition partitioning. The nodal points interior to the substructures (subset I) are ordered first, followed by those on the interface Γ (subset Γ). Similarly, for the local stiffness matrix relative to a substructure Ω_i, we have

$$A^{(i)} = \begin{pmatrix} A_{II}^{(i)} & A_{I\Gamma}^{(i)} \\ A_{\Gamma I}^{(i)} & A_{\Gamma\Gamma}^{(i)} \end{pmatrix}.$$

First, the unknowns in the interior of the substructures are eliminated by block Gaussian elimination. In this step, the Schur complement $S = S_{NN}$ with respect to the interior variables is formed. The resulting linear system for the nodal values on Γ can be written as

$$S_{NN}\, u_\Gamma = g_\Gamma. \tag{3}$$

Given the local Schur complement associated to the substructure Ω_i

$$S_i = A_{\Gamma\Gamma}^{(i)} - A_{\Gamma I}^{(i)} {A_{II}^{(i)}}^{-1} A_{I\Gamma}^{(i)} \tag{4}$$

and the local right-hand side

$$g_{\Gamma_i} = b_{\Gamma_i} - A_{\Gamma I}^{(i)} {A_{II}^{(i)}}^{-1} b_I^{(i)},$$

the global Schur complement can be written as

$$S = S_{NN} = \sum_{i=1}^{N} R_i^T S_i R_i \tag{5}$$

and the corresponding right-hand side g_Γ as

$$g_\Gamma = \sum_{i=1}^{N} R_i^T g_{\Gamma_i}\,, \tag{6}$$

where the restriction matrix R_i is a matrix of zeros and ones which extracts the variables on the local interface Γ_i from a vector of nodal values on Γ.

The Balancing Neumann-Neumann preconditioner $\hat{S}^{-1}$ [25] gives a preconditioned operator P_{NN} of the following form

$$P_{NN} = \hat{S}^{-1} S_{NN} = P_0 + (I - P_0)(\sum_{i=1}^{N} P_i)(I - P_0). \tag{7}$$

Here P_0 is associated to a low dimensional global coarse problem, whereas each operator P_i is associated to one substructure. More precisely, the local operators P_i are defined as:

$$P_i = R_i^T D_i S_i^\dagger D_i R_i S_{NN}, \tag{8}$$

where the matrices D_i are diagonal and $S_i^\dagger$ denotes either the inverse of S_i, if S_i is non-singular as for reaction-diffusion problems or for subdomains that touch $\partial\Omega$, or a pseudoinverse of S_i, if S_i is singular as for floating domains and purely diffusive problems. In our experiments we employ the Moore-Penrose pseudoinverse in [17]. In order to define the matrices $\{D_i\}$, we need to introduce a weighted counting function δ_i, which is associated to Ω_i and is piecewise linear on Γ_i; cf. [11, 12, 25, 32, 37]. It is defined for $\gamma \in [1/2, \infty)$ and, is determined by a sum of contributions from Ω_i and its relevant next neighbors,

$$\delta_i(x_l) = \sum_{j \in \mathcal{N}_{x_l}} \left(a_{ll}^{(j)} / a_{ll}^{(i)} \right)^\gamma, \quad x_l \in \Gamma_{i,h}\,, \tag{9}$$

where $a_{ll}^{(i)}$ denotes the l-th element of the diagonal of the local stiffness matrix $A^{(i)}$ and $\mathcal{N}_{x_l}$, $x_l \in \Gamma_h$, is the set of indices j of the subregions such that $x_l \in \Gamma_{j,h}$. In case $c = 0$, we choose ρ_i and ρ_j instead of $a_{ll}^{(i)}$ and $a_{ll}^{(j)}$. We have chosen $\gamma = 1$ for our numerical experiments. The pseudoinverses $\delta_i^\dagger$ are defined, for $x \in \Gamma_{i,h}$, by

$$\delta_i^\dagger(x) = \delta_i^{-1}(x), \quad x \in \Gamma_{i,h}. \tag{10}$$

We note that these functions provide a partition of unity:

$$\sum_{i=1}^{N} R_i^T {\delta_i}^\dagger(x) \equiv 1. \tag{11}$$

Let D_i be the diagonal matrix with elements $\delta_i^\dagger(x)$ corresponding to the nodes in $\Gamma_{i,h}$.

The coarse space is defined as

$$V_0 = \text{span}\{R_i^T \delta_i^\dagger\},$$

where the span is taken over at least all the floating subdomains. We denote by R_0^T the prolongation from the coarse to the global space. In analogy with (8), the coarse operator P_0 is defined as:

$$P_0 = R_0^T S_0^{-1} R_0 S_{NN}, \tag{12}$$

where $S_0 = R_0 S_{NN} R_0^T$ denotes the restriction of S_{NN} to that coarse space. We refer the reader to [44] for more details. In this work, we have only considered *exact* solvers for the local and global problems. Consequently, P_0 is an orthogonal projection; cf. [41].

5.2.2 Algorithm

According to (3) and (7), the preconditioned system can be written in the following form:

$$P_{NN} u = \hat{S}^{-1} g_\Gamma. \tag{13}$$

Since P_0 is a projection, we have

$$P_0(I - P_0) = 0.$$

Thus a decomposition of the exact solution u of (13) as

$$u = P_0 u + w, \qquad P_0 u = R_0^T S_0^{-1} R_0 g_\Gamma, \tag{14}$$

with $w \in Range(I - P_0)$, leads to the following new formulation of (13):

$$(I - P_0)(\sum_{i=1}^{N} P_i)(I - P_0) w = \hat{S}^{-1} g_\Gamma - P_0 u, \qquad w \in Range(I - P_0). \tag{15}$$

One can easily check that $S_{NN} P_0 = P_0^T S_{NN}$, and thus the matrix in (15) can also be written as

$$(I - P_0)(\sum_{i=1}^{N} P_i)(I - P_0) = \left[(I - P_0)(\sum_{i=1}^{N} R_i^T D_i S_i^\dagger D_i R_i)(I - P_0^T)\right] S_{NN},$$

which gives the expression of the preconditioner $\hat{S}^{-1}$. Consequently, the Balancing Neumann-Neumann method reduces to a projected preconditioned Conjugate Gradient method in the space $Range(I - P_0)$ applied to the system:

$$\left[(I - P_0)(\sum_{i=1}^{N} R_i^T D_i S_i^\dagger D_i R_i)(I - P_0^T)\right] S_{NN}\, w = \hat{S}^{-1} g_\Gamma - P_0 u \tag{16}$$

if an initial guess $u_0 = P_0 u + \tilde{w}$, with $\tilde{w} \in Range(I - P_0)$, is chosen. The projected Conjugate Gradient method is presented in Table 1. In this table $\langle \cdot, \cdot \rangle$ denotes the Euclidean inner product. Thanks to (14) and to the choice of u_0, the first projection step, corresponding to the application of $I - P_0^T$, can be omitted in practice.

1. Initialize

$$u_0 = R_0^T S_0^{-1} R_0 g_\Gamma + \tilde{w}, \quad \tilde{w} \in Range(I - P_0)$$
$$q_0 = g_\Gamma - S_{NN}\, u_0$$

2. Iterate $j = 1, 2, \cdots$ until convergence

$$\begin{aligned}
\text{Project:} \quad & w_{j-1} = (I - P_0^T) q_{j-1} \\
\text{Precondition:} \quad & z_{j-1} = \sum_{i=1}^{N} R_i^T D_i S_i^\dagger D_i R_i\, w_{j-1} \\
\text{Project:} \quad & y_{j-1} = (I - P_0) z_{j-1} \\
& \beta_j = \langle y_{j-1}, w_{j-1} \rangle / \langle y_{j-2}, w_{j-2} \rangle \quad [\beta_1 = 0] \\
& p_j = y_{j-1} + \beta_j p_{j-1} \quad [p_1 = y_0] \\
& \alpha_j = \langle y_{j-1}, w_{j-1} \rangle / \langle p_j, S_{NN}\, p_j \rangle \\
& u_j = u_{j-1} + \alpha_j\, p_j \\
& q_j = q_{j-1} - \alpha_j S_{NN}\, p_j
\end{aligned}$$

Table 1: Balancing Neumann-Neumann algorithm.

We remark that the matrices S_{NN} and $S_i^\dagger$ do not need to be calculated in practice. The action of S_{NN} on a vector requires the solution of a Dirichlet problem on each substructure (application of the inverse of $A_{II}^{(i)}$), while the action of $S_i^\dagger$ can be calculated by applying a pseudo-inverse of $A^{(i)}$ to a suitable vector, corresponding to the solution of a Neumann problem; see [41, Chap 4.]. Thus one step of the algorithm in Table 1 involves one application of P_0, the solution of local Neumann problems on each substructure ($S_i^\dagger$) and the solution of local Dirichlet problems (S_{NN}). Since the application of P_0 also involves an application of S_{NN} and the solution of a coarse problem, the total amount of work per step is given by one Neumann and two Dirichlet problems on each substructure and one coarse problem.

5.2.3 Condition number bound

A bound for the condition number of the preconditioned operator P_{NN} restricted to the subspace $Range(I - P_0)$, to which the iterates are confined, has been proven in [44] for the case $(\rho_x, \rho_y) = (\rho, \rho)$, $(\varepsilon_x, \varepsilon_y) = (1, 1)$, and $c = 0$. We have

$$\kappa(P_{NN}) \leq C\,(1 - \sigma)^{-4} \left(1 + \log\left(\frac{k}{1 - \sigma}\right)\right)^2, \tag{17}$$

where the constant C is independent of the spectral polynomial degree k, the level of refinement n, the mesh grading factor σ, the coefficients ρ, and the

diameters of the substructures H_i. We note that $\kappa(P_{NN})$ does not depend on the number of substructures or the aspect ratio of the mesh and only depends polylogarithmically on the spectral polynomial degree k as in the p version on shape-regular meshes. Finally, we remark that σ is bounded away from one and zero in practice.

5.3 One-level FETI methods

FETI methods were first introduced in [16]. Since then, considerable work has been done on FETI methods and many variants and improvements have been proposed. We refer to [15] for a detailed introduction and to [22, 27] for the analysis of one-level FETI methods.

5.3.1 Derivation

For brevity, we only present the one-level FETI method in the case of purely diffusive problems. We refer to section 5.3.4 for some details in the case of reaction-diffusion problems, i.e., when the local matrices $A^{(i)}$ are invertible. Instead of solving the Schur complement system (3), a FETI method uses a space of discontinuous functions across the interface Γ. The continuity of the solution is then enforced by using a vector of Lagrange multipliers and this leads to the saddle-point formulation

$$\left.\begin{aligned} S_F u_F + B^T \lambda &= g_F \\ B u_F &= 0 \end{aligned}\right\}, \tag{18}$$

with

$$u_F = \begin{bmatrix} u^{(1)} \\ u^{(2)} \\ \vdots \\ u^{(N)} \end{bmatrix}, \; S_F = \begin{bmatrix} S_1 & O & \cdots & O \\ O & S_2 & \ddots & \vdots \\ \vdots & \ddots & \ddots & O \\ O & \cdots & O & S_N \end{bmatrix}, \; g_F = \begin{bmatrix} g^{(1)} \\ g^{(2)} \\ \vdots \\ g^{(N)} \end{bmatrix}$$

where each diagonal block of S_F is a Schur complement matrix of the form (4) and B a matrix consisting of $(-1, 0, 1)$ that enforces the continuity of the solution at the interfaces between the substructures. In this work, non-redundant Lagrange multipliers have been considered; thus the matrix B has full rank. In addition, we denote by R the full-column rank matrix built from all the non-void null space elements of S_F, i.e., those S_i corresponding to floating subdomains:

$$R = \begin{bmatrix} r_1 & O & \cdots & O \\ O & r_2 & \ddots & \vdots \\ \vdots & \ddots & \ddots & O \\ O & \cdots & O & r_{N_f} \end{bmatrix}$$

where N_f denotes the number of floating domains. In fact, for Problem (M) the columns of R span the kernel of S_F. We also define $G = BR$. In the next step we eliminate the primal variable u_F in (18) and derive an equation for the Lagrange multiplier λ only. This leads to

$$u_F = {S_F}^{\dagger}(g_F - B^T\lambda) + R\alpha, \quad (g_F - B^T\lambda) \perp Kernel(S_F),$$

with $S_F^{\dagger}$ denoting a pseudo-inverse of S_F and

$$\left.\begin{array}{rcl} F\lambda - G\alpha & = & d \\ G^T\lambda & = & e \end{array}\right\}, \tag{19}$$

with $F = B{S_F}^{\dagger}B^T$, $d = B{S_F}^{\dagger}g_F$, and $e = R^T g_F$. After introducing a suitable orthogonal projection operator P onto the orthogonal complement of $Range(G)$ and a preconditioner M^{-1} (both defined below), the one-level FETI method reduces to the preconditioned Conjugate Gradient method applied in the space of Lagrange multipliers to the following system:

$$PM^{-1}P^TF\lambda = PM^{-1}P^Td, \tag{20}$$

with an initial approximation λ_0 that satisfies the second of (19). We can choose

$$\lambda_0 = QG(G^TQG)^{-1}R^Tg_F + \tilde{w}, \qquad \tilde{w} \in Range(P)\,, \tag{21}$$

where Q is a symmetric invertible matrix to be chosen. Here P is an orthogonal projection operator defined as $P = I - QG(G^TQG)^{-1}G^T$.

Many choices have been proposed for the preconditioner M^{-1} and the matrix Q. The choice

$$M^{-1} = (BD^{-1}B^T)^{-1}BD^{-1}S_FD^{-1}B^T(BD^{-1}B^T)^{-1}, \quad Q = M^{-1} \tag{22}$$

ensures a condition number that is independent of the jumps in the coefficients; see [22]. Here D is a block diagonal matrix: each block D_i corresponds to one substructure Ω_i, and is equal to the local scaling matrix introduced in section 5.2.1.

5.3.2 Algorithm

The FETI method is a projected preconditioned Conjugate Gradient method in the space of Lagrange multipliers $Range(P)$ applied to the system (20) with an initial approximation chosen as in (21). This algorithm is given in Table 2. Note that due to the choice of the initial iterate λ_0, the first projection step (application of P^T) can be omitted in practice.

1. Initialize

$$\lambda_0 = QG(G^TQG)^{-1}R^T g_F + \tilde{w}, \quad \tilde{w} \in Range(P)$$
$$q_0 = d - F\,\lambda_0$$

2. Iterate $j = 1, 2, \cdots$ until convergence

$$\begin{aligned}
\text{Project:} \quad & w_{j-1} = P^T q_{j-1} \\
\text{Precondition:} \quad & z_{j-1} = M^{-1} w_{j-1} \\
\text{Project:} \quad & y_{j-1} = P z_{j-1} \\
& \beta_j = \langle y_{j-1}, w_{j-1}\rangle / \langle y_{j-2}, w_{j-2}\rangle \quad [\beta_1 = 0] \\
& p_j = y_{j-1} + \beta_j p_{j-1} \quad [p_1 = y_0] \\
& \alpha_j = \langle y_{j-1}, w_{j-1}\rangle / \langle p_j, F p_j\rangle \\
& \lambda_j = \lambda_{j-1} + \alpha_j p_j \\
& q_j = q_{j-1} - \alpha_j F p_j
\end{aligned}$$

Table 2: FETI algorithm.

We remark that F and M^{-1} do not need to be calculated in practice. The action of M^{-1} on a vector basically requires the solution of a Dirichlet problem on each substructure (application of S_F, and thus the S_i). Indeed, the matrix $BD^{-1}B^T$ is block diagonal: each block corresponds to a node on Γ and its dimension is equal to the number of constraints imposed on that node by the second of (18): it can then be easily inverted. The action of F can be calculated by solving Neumann problems on the substructures (application of the pseudoinverses $S_i^\dagger$). Finally, one application of P is required at each step and involves the solution of a coarse problem (application of $(G^TQG)^{-1}$) and an additional application of M^{-1}. The total amount of work per step is then comparable to that of the Neumann-Neumann algorithm and requires the solution of one Neumann and two Dirichlet problems on each substructure and one coarse problem.

5.3.3 Condition number bound

We denote by $P_F = PM^{-1}P^TF$ the preconditioned operator in system (20). A bound for the condition number of P_F restricted to the appropriate subspace $Range(P)$ to which the iterates are confined has been proven in [44] for the case $(\rho_x, \rho_y) = (\rho, \rho)$, $(\varepsilon_x, \varepsilon_y) = (1, 1)$ and $c = 0$:

$$\kappa(P_F) \leq C\,(1-\sigma)^{-4}\,\left(1 + \log\left(\frac{k}{1-\sigma}\right)\right)^2. \tag{23}$$

We stress the fact that the constant in the estimate is independent of k, n, σ, the coefficients ρ and the diameters H_i of the substructures. Note that $\kappa(P_F)$ does not depend on the number of substructures or the aspect ratio of the mesh and only depends polylogarithmically on the spectral polynomial degree.

5.3.4 Reaction-diffusion problems

In the case of reaction-diffusion problems, the local Schur complements (4) and thus S_F are always non-singular. Thus the modification for one-level FETI methods proposed in [13] has been employed. The system for the Lagrange multiplier λ (19) is now replaced by $F\lambda = d$ with $F = BS_F^{-1}B^T$ and $d = BS_F^{-1}g_F$. Following [43], a new projection operator P can be defined as

$$P = I - QG(G^TQFQG)^{-1}G^TQF.$$

With these new notations, the preconditioned system can be written as in (20) with now an initial guess of the form:

$$\lambda_0 = QG(G^TQFQG)^{-1}G^TQd + \tilde{w}, \quad \text{with} \quad \tilde{w} \in Range(P).$$

The same preconditioner M^{-1} and scaling matrix Q as in (22) are employed. Our domain decomposition operators have condition numbers that are independent of the jumps in the coefficients; see section 7.6.2.

We note that a new class of FETI methods has recently been introduced, the so-called dual-primal FETI methods; see [14]. In two dimensions variables associated to the vertices of the substructures are eliminated together with the internal degrees of freedom. The constrained problem in (18) only involves degrees of freedom in the interior of the edges of the subdomains and the resulting Schur complement S_F is now invertible. The equation for the Lagrange multiplier λ is now: $F\lambda = d$, instead of (19). The same preconditioner M^{-1}, which gives the preconditioned operator $M^{-1}F$. We refer to [28, 23] for the analysis of certain dual primal FETI methods. One of the main advantages of dual-primal FETI methods is that they can be implemented in exactly the same way for purely diffusive and reaction-diffusion problems, since the local Schur complements are always invertible. In addition, they do not require the introduction of the projection P and thus of a scaling matrix Q. These methods can be defined for our approximations as well and the proof can be carried out as in [28, 23].

6 Remarks on condition numbers

In this section we make some remarks on what type of condition number bounds can be expected for S and some iterative substructuring methods. Our upper bounds are then confirmed by the numerical experiments in section 7.

We consider a simple Laplace problem, corresponding to the choice $(\varepsilon_x, \varepsilon_y) = (1,1)$, $(\rho_x, \rho_y) = (1,1)$, and $c = 0$ in Problem (M). The analysis in [29] for general shape-regular, quasi-uniform meshes and nodal basis functions on Gauss-Lobatto nodes can be applied to the case $\mathcal{T}^{DD} = \mathcal{T}^0 = \mathcal{T}$ and ensures a growth like k/h^2 for $\kappa(S)$, where h denotes the diameter of the fine triangulation; cf. section 7.1 and Figure 1. We note that in this case $H = h$. On the other hand, following [10], where estimates for h approximations are provided, we expect a growth like $k/(hH)$, for the case of shape-regular and quasi-uniform meshes and more general partitions into subdomains.

For meshes that are not shape regular or quasi-uniform, h needs to be replaced by a characteristic minimum size of the elements. For our geometrically refined meshes we have $h \sim \sigma^n H$, and thus

$$\kappa(S) \leq C\frac{k}{hH} \sim C\frac{k}{H^2}(1/\sigma)^n \sim C\frac{k}{H^2}(1/\sigma)^k, \tag{24}$$

with $n \sim k$ as required for exponential convergence in the presence of singularities. We then expect that the condition number of S grows exponentially with k and linearly in the number of subdomains ($N \sim (1/H)^2$). This is consistent with the results in section 7.4; see Figure 5 in particular.

For quasi-uniform and shape-regular meshes iterative substructuring methods generally lead to condition numbers varying as a power of $\log(kH/h)$ for hp finite element approximations; see, e.g., [2, 4, 9, 18, 19, 20, 31]. Such estimates usually rely on stable decompositions of finite element functions into terms associated to geometrical objects. In two dimensions they typically involve terms associated to edges and *internal* vertices; see, e.g., [44, Eq. 29]. When the local meshes are not quasi-uniform, the mesh size h in the ratio must be replaced by a characteristic minimum size of the elements *in the neighborhood* of internal vertices. Property 4.2 ensures that anisotropic refinement is only carried out towards $\partial\Omega$ and thus far from the internal vertices of the subdomains. By construction, in the neighborhood of a vertex, the ratio H/h is bounded by $(1-\sigma)^{-1}$. This explains the bounds for the condition numbers of our preconditioned Neumann-Neumann and FETI operators in (17) and (23). These estimates are confirmed by our numerical experiments.

In our tests, we have also considered more general meshes than those introduced in section 4. Indeed, certain problems may require geometric refinement in the interior of the computational domain; see section 7.5. In this case, $h \sim H\sigma^n$ and we thus expect

$$\kappa(P_{NN}) \sim \kappa(P_F) \leq C\,\left(1+\log\left(\frac{kH}{h}\right)\right)^2 \sim C\,\left(1+\log\left(k\sigma^{-n}\right)\right)^2 \leq C\,k^2,$$

with $n \sim k$. We note that the condition number bound is in this case quadratic with the polynomial degree, but it provides however an improvement over the exponentially varying one of the original Schur complement. Indeed, the results

in section 7.5 are consistent with a *linear* growth in k and very small iteration counts are obtained in practice.

7 Numerical experiments

The purpose of this section is to investigate the convergence behaviour of Balancing Neumann-Neumann (denoted by **NN**) and of one-level FETI (denoted by **FETI**) methods when applied to six sets of elliptic problems - all derived from Problem (M). Particular attention is devoted to a comparison between the condition numbers $\kappa(P_{NN})$ and $\kappa(P_F)$ obtained numerically and the corresponding theoretical bounds (17) and (23). The six problems considered are derived from Problem (M) defined in section 2 by an appropriate choice of the coefficients $(\varepsilon_x, \varepsilon_y, \rho_x, \rho_y, c)$. The first three test cases (Problems I, II, III) are standard test problems for domain decomposition preconditioners; see [25, 33, 41]. These problems defined on *shape-regular* and *uniform meshes* have been chosen here as a first evaluation step before tackling more involved problems. The last three test cases (Problems IV, V, VI) are defined on *highly anisotropic meshes* (except those in section 7.6.2). These more difficult problems have been chosen as a natural extension of Problems I and II approximated on highly anisotropic meshes.

Results for the two unpreconditioned systems ($\kappa(S_{NN})$ and $\kappa(F)$, respectively) have also been included to provide an idea of the difficulty of the problems. These condition numbers are obtained by computing the eigenvalues of the tridiagonal symmetric Lanczos matrix built by the Conjugate Gradient (CG) iterative process; see [7] for details. The minimum and maximum eigenvalues (λ_{min} and λ_{max}, respectively) are also reported. The number of iterations It to reduce the Euclidean norm of the residual $\|r\|_2$ by fourteen orders of magnitude

$$\|r_{It}\|_2/\|r_0\|_2 \leq 10^{-14} \tag{25}$$

is also reported. We have chosen this rather strict stopping criterion, since the primal solution in the FETI formulation is only continuous at convergence. As initial guess, a zero initial field ($\tilde{w} = 0$ in Tables 1 and 2) is used for all problems. Finally in these numerical experiments u_D has been chosen as an analytical function that leads to non-homogeneous Dirichlet boundary conditions. All the numerical experiments presented here have been carried out in Matlab 6.1.

7.1 Problem I: a Laplace problem

In order to have reference results for later comparison (Problem IV), we have first considered the Laplace operator with inhomogeneous Dirichlet boundary conditions ($(\varepsilon_x, \varepsilon_y) = (1, 1), (\rho_x, \rho_y) = (1, 1), c = 0$ in Problem (M)):

$$\begin{array}{ll} -\Delta u = f, & \text{in } \Omega, \\ u = u_D, & \text{on } \partial\Omega. \end{array} \tag{26}$$

The source term f is derived in such a way that u_D is the exact solution of this problem. The unrefined $\mathcal{T}$ mesh is of Cartesian type and consists of $N_x \times N_y$ rectangles. Since in Problems I, II, and III unrefined meshes are used, $\mathcal{T}^{DD}$ and $\mathcal{T}$ are identical. Thus the total number of substructures is $N = N_x \times N_y$.

The results for the Balancing Neumann-Neumann and FETI preconditioners are shown in Table 3 and Table 4, respectively. In the upper half of the tables, the number of substructures is kept fixed ($N_x \times N_y = 3 \times 3$), while the spectral polynomial degree k is varying from 2 to 12. In the lower half the spectral degree k is fixed to 4, while the number of substructures is increased from 2×2 to 12×12. The first four columns report the iteration counts required to satisfy the stopping criterion (25), the maximum and minimum eigenvalues, and the condition number for the unpreconditioned operators S_{NN} and F. The next four columns show the same data, when Balancing Neumann-Neumann or one-level FETI methods are employed with CG.

The condition number of the unpreconditioned Schur operator $\kappa(S_{NN})$ is plotted in Figure 1. As expected (cf. section 6), $\kappa(S_{NN})$ grows like k when the number of substructures is fixed (Figure 1, right), while $\kappa(S_{NN})$ grows like $1/H^2$ when the spectral degree is fixed (Figure 1, left). Whatever the choice of the preconditioner, the iteration count for preconditioned CG appears to be bounded independently of $N_x \times N_y$; see lower parts of Tables 3 and 4. The condition numbers $\kappa(P_{NN})$ and $\kappa(P_F)$ are plotted in Figure 2 versus the spectral polynomial degree. As expected, the growth is quadratically in $\log(k)$. Also note that the minimum eigenvalues of P_{NN} and P_F satisfy the lower bounds proven in [44, Lemmas 6.2 and 6.4], respectively. Unless otherwise stated, this feature will also be true for the other problems investigated in this paper. Note finally that the condition numbers presented in Table 3 are in good agreement with those obtained in [33, Table 6.1] for the same problem. As for Table 4, we are unaware of any theoretical or numerical study on FETI methods for spectral element approximations.

7.2 Problem II: a Laplace problem with jump coefficients

The theoretical bounds for the condition number provided in (17) and (23) are independent of arbitrary jumps on the coefficients between the substructures. The purpose of this test case, also considered in [25] is to check this property. Therefore the following problem, corresponding to the choice $(\varepsilon_x, \varepsilon_y) = (1, 1), c = 0, f = 1$ in Problem (M), has been considered

$$\begin{array}{ll} -\nabla \cdot (\rho \nabla u) = 1, & \text{in } \Omega, \\ u = u_D, & \text{on } \partial\Omega, \end{array} \tag{27}$$

where the coefficient $\rho = \rho_x = \rho_y$ possibly changes between the substructures by many orders of magnitude. Non-homogeneous Dirichlet boundary conditions

Fixed number of substructures $N_x \times N_y = 3 \times 3$								
	No preconditioning				**NN**			
k	It	λ_{max}	λ_{min}	$\kappa(S_{NN})$	It	λ_{max}	λ_{min}	$\kappa(P_{NN})$
2	9	5.3161	0.6667	7.9741	6	1.076	1	1.076
3	19	5.6508	0.3964	14.2544	9	1.4364	1	1.4364
4	26	5.7291	0.28	20.4629	10	1.7542	1	1.7542
5	31	5.7737	0.2157	26.7612	11	2.1137	1	2.1137
6	34	5.8029	0.1752	33.1169	12	2.4471	1	2.4471
7	38	5.8264	0.1474	39.5316	13	2.7688	1	2.7688
8	42	5.8465	0.1271	45.995	13	3.07	1	3.07
9	45	5.8644	0.1117	52.5011	13	3.3575	1	3.3575
10	48	5.8807	0.0996	59.0453	14	3.629	1	3.629
11	52	5.896	0.0898	65.624	14	3.8884	1	3.8884
12	55	5.9103	0.0818	72.2349	14	4.1352	1	4.1352
Fixed spectral degree $k = 4$								
	No preconditioning				**NN**			
$N_x \times N_y$	It	λ_{max}	λ_{min}	$\kappa(S_{NN})$	It	λ_{max}	λ_{min}	$\kappa(P_{NN})$
2 x 2	10	5.5968	0.544	10.2891	3	1.5034	1	1.5034
3 x 3	26	5.7291	0.28	20.4629	10	1.7542	1	1.7542
4 x 4	36	5.7773	0.1655	34.9023	14	1.8179	1	1.8179
5 x 5	45	5.8	0.1084	53.5172	16	1.8528	1	1.8528
6 x 6	57	5.8124	0.0762	76.287	16	1.8725	1	1.8725
7 x 7	67	5.8199	0.0564	103.2052	16	1.8854	1	1.8854
8 x 8	76	5.8248	0.0434	134.269	16	1.8939	1	1.8939
9 x 9	85	5.8281	0.0344	169.477	16	1.8998	1	1.8998
10 x 10	94	5.8305	0.0279	208.8288	16	1.9041	1	1.9041
11 x 11	103	5.8323	0.0231	252.3238	16	1.9073	1	1.9073
12 x 12	111	5.8336	0.0194	299.9618	16	1.9098	1	1.9098

Table 3: **Laplace problem**. Conjugate Gradient method for the Schur complement system without preconditioning and with Neumann-Neumann preconditioner: iteration counts, maximum and minimum eigenvalues, and condition numbers versus polynomial degree and number of subdomains, respectively.

u_D have also been considered. Given a partition of Ω into $N_x \times N_y$ substructures ($\mathcal{T} = \mathcal{T}^{DD} = N_x \times N_y$), a checkerboard distribution is considered for ρ which is equal to either ρ_1 or ρ_2 as in [25].

Fixed number of substructures $N_x \times N_y = 3 \times 3$								
	No preconditioning				**FETI**			
k	It	λ_{max}	λ_{min}	$\kappa(F)$	It	λ_{max}	λ_{min}	$\kappa(P_F)$
2	24	8.309	0.57385	14.4793	9	2.0516	1.0002	2.0512
3	36	11.089	0.62896	17.6308	11	2.7284	1.0001	2.7281
4	39	13.685	0.64515	21.2113	12	3.4415	1.0002	3.4409
5	42	16.263	0.65642	24.7761	12	4.0378	1.0003	4.0364
6	44	18.867	0.65997	28.5881	12	4.5902	1.0003	4.5888
7	48	21.51	0.66639	32.2776	14	5.0849	1.0001	5.0843
8	47	24.186	0.66492	36.3747	13	5.5443	1.0007	5.5404
9	52	26.892	0.67048	40.1091	14	5.9669	1.0006	5.9633
10	50	29.622	0.66676	44.427	14	6.3628	1.0011	6.3558
11	56	32.37	0.67049	48.2788	15	6.7327	1.0009	6.7267
12	53	35.134	0.66716	52.6613	15	7.0821	1.0016	7.0708
Fixed spectral degree $k = 4$								
	No preconditioning				**FETI**			
$N_x \times N_y$	It	λ_{max}	λ_{min}	$\kappa(F)$	It	λ_{max}	λ_{min}	$\kappa(P_F)$
2 x 2	15	10.846	0.65997	16.4338	4	2.2515	1	2.2515
3 x 3	39	13.685	0.64515	21.2113	12	3.4415	1.0002	3.4409
4 x 4	49	14.076	0.63808	22.0603	16	3.0693	1.0002	3.0686
5 x 5	61	14.443	0.45086	32.0348	18	3.0485	1.0006	3.0467
6 x 6	69	14.652	0.34379	42.618	19	2.9854	1.0004	2.9844
7 x 7	75	14.777	0.29059	50.852	20	2.9877	1.0004	2.9864
8 x 8	81	14.858	0.26057	57.0227	19	2.9769	1.0004	2.9758
9 x 9	88	14.913	0.24195	61.6358	19	2.9768	1.0004	2.9757
10 x 10	92	14.952	0.2296	65.1196	20	2.9769	1.0003	2.9759
11 x 11	97	14.98	0.22098	67.7892	20	2.9771	1.0003	2.9761
12 x 12	101	15.001	0.21471	69.8672	20	2.9768	1.0003	2.9759

Table 4: **Laplace problem**. Conjugate Gradient method for the FETI system without and with preconditioning: same legend as Table 3.

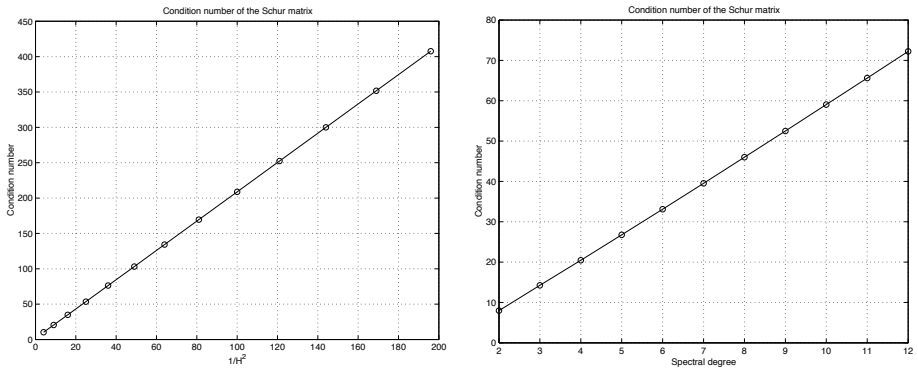

Figure 1: **Laplace problem**. Dependence of the condition number of the Schur complement matrix $\kappa(S_{NN})$ on the number of substructures (left) and the spectral degree (right) (results from Table 3).

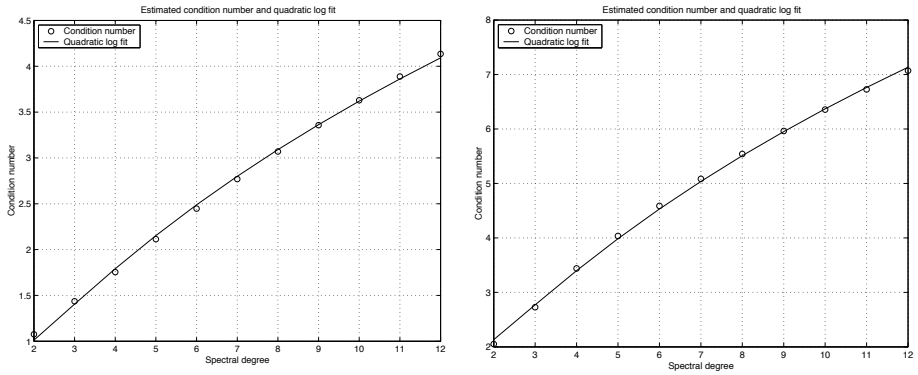

Balancing Neumann-Neumann FETI

Figure 2: **Laplace problem**. Estimated condition numbers (circles) and least-square second order logarithmic polynomial fit (solid line) versus the spectral degree for the Balancing Neumann-Neumann (left, results from Table 3) and the FETI preconditioned operators (right, results from Table 4).

7.2.1 Fixed jumps between the substructures

In this part, we fix the values $\rho_1 = 10^{-3}$ and $\rho_2 = 10^3$. We consider four different partitions with $N_x \times N_y = (2 \times 2, 3 \times 3, 4 \times 4, 5 \times 5)$ and we vary the spectral polynomial degree k from 2 to 12 as in the previous experiments. For brevity, the results are not presented here in form of tables. As before, the condition numbers $\kappa(P_{NN})$ and $\kappa(P_F)$ are plotted in Figure 3 versus the spectral degree for each partition and for both preconditioned operators. The condition numbers $\kappa(P_{NN})$ and $\kappa(P_F)$ grow as the squared logarithm of the spectral degree

k and are bounded independently of the number of subdomains. This is again in agreement with the bounds (17) and (23). Despite the bad conditioning of the original system ($\rho_2/\rho_1 = 10^6$), Balancing Neumann-Neumann and one-level FETI methods provide very good preconditioners in this case.

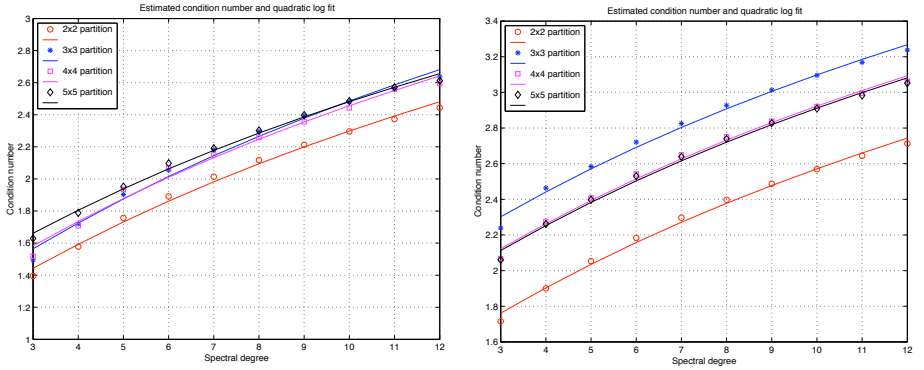

Balancing Neumann-Neumann FETI

Figure 3: **Laplace problem with jump coefficients. Case of $\rho_1 = 10^{-3}$ and $\rho_2 = 10^3$.** Estimated condition numbers (circles) and least-square second order logarithmic polynomial fit (solid line) versus the spectral degree for the Balancing Neumann-Neumann (left) and the FETI (right) methods.

7.2.2 Variable coefficient jumps

In this part, the spectral polynomial degree k is fixed to 10. For two different partitions $N_x \times N_y = (3\times 3, 5\times 5)$, we have investigated the influence of the jump ρ_2/ρ_1 on the convergence behaviour of Balancing Neumann-Neumann and one-level FETI methods. In this experiment, ρ_1 is fixed to 1, whereas ρ_2 is varying from 1 to 10^6. A checkerboard distribution has also been used.

The results are presented in Table 5. Whatever the choice of the preconditioner, the number of preconditioned CG iterations in order to satisfy the stopping criterion (25) is bounded independently of the ratio ρ_2/ρ_1, in agreement with the bounds (17) and (23). Note that a smallest eigenvalue equal to one is not always found for some values of the jump. This may be due to a loss of orthogonality in the iterates of the CG iteration; see [6].

7.3 Problem III: a Laplace problem with anisotropic diffusion

Problems I and II are considered as standard test problems for iterative substructuring methods. In addition we have investigated the Laplace problem with

Fixed number of substructures $N_x \times N_y = 3 \times 3$								
	NN				**FETI**			
ρ_2	It	λ_{max}	λ_{min}	$\kappa(P_{NN})$	It	λ_{max}	λ_{min}	$\kappa(P_F)$
1	14	3.629	1	3.629	14	6.3628	1.0011	6.3557
10	12	2.8612	1	2.8612	12	4.2857	1.0007	4.2828
10^2	9	2.5372	1	2.5372	10	3.234	1.0001	3.2337
10^3	8	2.4877	1	2.4877	8	3.1098	1	3.1097
10^4	7	2.4825	1	2.4825	7	3.0972	1	3.0972
10^5	6	2.482	1	2.482	7	3.0959	1	3.0959
10^6	7	2.482	1	2.482	6	3.0958	1	3.0958
Fixed number of substructures $N_x \times N_y = 5 \times 5$								
	NN				**FETI**			
ρ_2	It	λ_{max}	λ_{min}	$\kappa(P_{NN})$	It	λ_{max}	λ_{min}	$\kappa(P_F)$
1	24	3.786	1	3.786	23	5.6907	1.0009	5.6856
10	19	2.9479	1	2.9479	20	3.9292	1.0006	3.9269
10^2	14	2.5198	1	2.5198	16	3.0279	1.0002	3.0273
10^3	12	2.4671	1	2.4671	13	2.9214	1.0001	2.9212
10^4	17	2.4614	0.96131	2.5605	12	2.9106	1.0001	2.9106
10^5	14	2.4612	0.99456	2.4746	12	2.9095	1.0001	2.9095
10^6	24	2.4617	0.9651	2.5508	13	2.9098	1.0001	2.9098

Table 5: **Laplace problem with jump coefficients. Case of $k = 10$ and $\rho_1 = 1$.** Conjugate Gradient method for the Balancing Neumann-Neumann and FETI methods: iteration counts, maximum and minimum eigenvalues, and condition numbers versus ρ_2.

anisotropic diffusion defined by $(\rho_x, \rho_y) = (1, 1), c = 0, f = 1$, and $(\varepsilon_x, \varepsilon_y) = (\varepsilon, 1)$ in Problem (M).

$$\begin{aligned} -\varepsilon \frac{\partial^2 u}{\partial x^2} - \frac{\partial^2 u}{\partial y^2} &= 1, \quad \text{in } \Omega, \\ u &= u_D, \qquad \text{on } \partial\Omega. \end{aligned} \tag{28}$$

In these experiments, ε is a small positive parameter. In the following we are interested in assessing the behaviour of the proposed preconditioners for small values of ε.

Note also that Problem III is equivalent to solve a standard Laplace problem on the following domain $\Omega_\varepsilon = [0, 1/\sqrt{\varepsilon}] \times [0, 1]$, i.e., for small parameters Ω_ε is a

thin domain. This kind of domain is needed e.g. in computational mechanics to capture boundary layer effects or in biomedical applications to compute viscous blood flows in large arteries; see, e.g., [34].

We have considered two partitions ($N_x \times N_y = 3 \times 1$ and $N_x \times N_y = 6 \times 1$) and have investigated the behaviour of the condition numbers $\kappa(P_{NN})$ and $\kappa(P_F)$ when varying the perturbation parameter ε for a fixed spectral degree $k = 4$. The results are collected in Tables 6 and 7 for the Balancing Neumann-Neumann and one-level FETI preconditioners, respectively. Note that both preconditioners are extremely efficient on this problem, since for moderate values of ε, they already tend to be direct solvers as expected in the limit case $\varepsilon = 0$. The same property holds when the partition is fixed and the spectral polynomial degree k is varying (the results are not presented here). Both preconditioners are therefore robust with respect to the perturbation parameter for this problem in case a partition of Ω into strips is employed. We note that FETI without preconditioning provides a fairly good performance when ε is close to zero, as opposed to the unpreconditioned Schur complement system.

7.4 Problem IV: a Laplace problem on a boundary layer mesh

So far, we have only considered model problems on uniform meshes and shown that, from Problems I, II and III, the numerical experiments are in agreement with the theoretical bounds (17) and (23). In the remainder of this paper, our goal is to investigate the convergence property on highly anisotropic meshes. The domain decomposition partition $\mathcal{T}^{DD}$ is now different from the refined mesh $\mathcal{T}$.

Problem IV is a natural extension of Problem I: it is a Laplace problem ($(\varepsilon_x, \varepsilon_y) = (1,1), (\rho_x, \rho_y) = (1,1), c = 0, f = 1$ in Problem (M)) with nonhomogeneous Dirichlet boundary conditions defined on a boundary layer mesh.

$$\begin{array}{ll} -\Delta u = 1, & \text{in } \Omega, \\ u = u_D, & \text{on } \partial\Omega. \end{array} \tag{29}$$

Here only a refinement toward the two intersecting edges $x = 0$ and $y = 0$ has been considered; see Figure 4. We note that this is a genuine *hp* approximation. As shown in [3, 5, 30, 39], in order to obtain exponential convergence in presence of singularities in polygonal domains, the number of layers n must be at least equal to the spectral degree k, thus better accuracy is achieved by simultaneously increasing the polynomial degree and the number of layers. In our experiments we have chosen $n = k$.

7.4.1 Fixed spectral degree

In this part, the spectral polynomial degree k is fixed to 4. Given a uniform macromesh $\mathcal{T}^0$ of size $N_x \times N_y$, we consider refinements with 4 layers in each

Fixed number of substructures $N_x \times N_y = 3 \times 1$								
	No preconditioning				**NN**			
ε	It	λ_{max}	λ_{min}	$\kappa(S_{NN})$	It	λ_{max}	λ_{min}	$\kappa(P_{NN})$
1	22	5.336	0.44784	11.9151	6	1.1268	1	1.1268
10^{-1}	22	3.0688	0.15677	19.5747	4	1.0007	1	1.0007
10^{-2}	22	2.8013	0.054723	51.1902	3	1	1	1
10^{-3}	22	2.7739	0.030654	90.4903	2	1	1	1
10^{-4}	22	2.7711	0.027647	100.2326	2	1	1	1
10^{-5}	22	2.7708	0.027338	101.3562	2	1	1	1
10^{-6}	22	2.7708	0.027307	101.4703	2	1	1	1
10^{-7}	22	2.7708	0.027304	101.4817	1	1	1	1
10^{-8}	22	2.7708	0.027303	101.4828	1	1	1	1
Fixed number of substructures $N_x \times N_y = 6 \times 1$								
	No preconditioning				**NN**			
ε	It	λ_{max}	λ_{min}	$\kappa(S_{NN})$	It	λ_{max}	λ_{min}	$\kappa(P_{NN})$
1	49	5.386	0.1301	41.399	12	2.14	1	2.14
10^{-1}	66	3.1314	0.060223	51.9968	7	1.0681	1	1.0681
10^{-2}	83	2.8633	0.025927	110.4379	3	1	1	1
10^{-3}	87	2.8359	0.0099745	284.3096	2	1	1	1
10^{-4}	77	2.8331	0.00719	394.0288	2	1	1	1
10^{-5}	67	2.8328	0.0068822	411.6134	2	1	1	1
10^{-6}	52	2.8328	0.0068509	413.4915	2	1	1	1
10^{-7}	50	2.8328	0.0068477	413.6805	1	1	1	1
10^{-8}	49	2.8328	0.0068474	413.6994	1	1	1	1

Table 6: **Laplace problem with anisotropic diffusion. Case of** $k = 4$. Conjugate Gradient method for the Schur complement system without preconditioning and with Neumann-Neumann preconditioner: iteration counts, maximum and minimum eigenvalues, and condition numbers versus the perturbation parameter.

direction (see Figure 4). Mesh grading factors $\sigma_x = 0.5$ and $\sigma_y = 0.5$ have been used. The non-uniform geometrically refined grid $\mathcal{T}$ contains $(N_x+4)\times(N_y+4)$ elements (see Fig. 4 for a partition with $N_x \times N_y = 12 \times 12$), whereas the subdomain partition $\mathcal{T}^{DD}$ has $N_x \times N_y$ substructures.

Table 8 and Table 9 show the results for the Neumann-Neumann and FETI preconditioners, respectively, for different partitions $\mathcal{T}^{DD}$. For both precondi-

Fixed number of substructures $N_x \times N_y = 3 \times 1$								
	No preconditioning				**FETI**			
ε	It	λ_{max}	λ_{min}	$\kappa(F)$	It	λ_{max}	λ_{min}	$\kappa(P_F)$
1	20	11.179	0.74974	14.9101	6	1.2602	1.0001	1.2602
10^{-1}	22	25.55	1.3036	19.6001	3	1.0014	1	1.0014
10^{-2}	22	73.096	1.428	51.1858	2	1	1	1
10^{-3}	18	130.49	1.442	90.489	2	1	1	1
10^{-4}	15	144.68	1.4435	100.2306	1	1	1	1
10^{-5}	11	146.32	1.447	101.1152	1	1	1	1
10^{-6}	8	146.48	1.5135	96.7833	1	1	1	1
10^{-7}	3	146.5	9.8775	14.8318	1	1	1	1
10^{-8}	1	1	1	1	1	1	1	1

Fixed number of substructures $N_x \times N_y = 6 \times 1$								
	No preconditioning				**FETI**			
ε	It	λ_{max}	λ_{min}	$\kappa(F)$	It	λ_{max}	λ_{min}	$\kappa(P_F)$
1	51	54.714	0.74284	73.6545	11	3.4988	1	3.4988
10^{-1}	53	68.505	1.2785	53.5808	6	1.1178	1	1.1178
10^{-2}	59	154.29	1.3973	110.4185	3	1.0001	1	1.0001
10^{-3}	57	401.29	1.4108	284.4416	2	1	1	1
10^{-4}	42	556.43	1.4128	393.8609	2	1	1	1
10^{-5}	28	581.24	1.4188	409.669	1	1	1	1
10^{-6}	19	583.87	1.4398	405.5268	1	1	1	1
10^{-7}	7	584.13	6.7258	86.8493	1	1	1	1
10^{-8}	1	581.75	581.75	1	1	1	1	1

Table 7: **Laplace problem with anisotropic diffusion. Case of** $k = 4$. Conjugate Gradient method for the FETI system without and with preconditioning: iteration counts, maximum and minimum eigenvalues, and condition numbers versus the perturbation parameter.

tioners, the iteration counts are uniformly bounded as the number of elements grow. Note that due to mesh refinement, the condition number of the Schur operators $\kappa(S_{NN})$ and $\kappa(F)$ are much higher than in Problem I; see section 6. Here the aspect ratio of the mesh is proportional to σ^{-k}. According to (24), $\kappa(S_{NN})$ should grow like H^{-2} for a fixed polynomial degree and this is confirmed by the results in Figure 5, left.

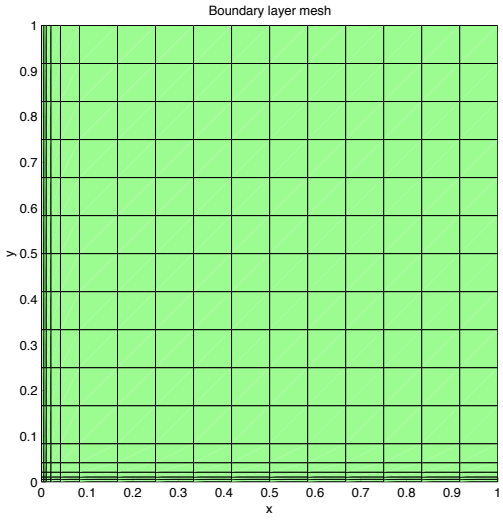

Figure 4: **Boundary layer mesh**. Refinement near two edges ($x = 0$ and $y = 0$) with 4 layers in each direction and mesh grading factors equal to $\sigma_x = 0.5$ and $\sigma_y = 0.5$. The macromesh is a Cartesian grid of size $N_x \times N_y = 12 \times 12$.

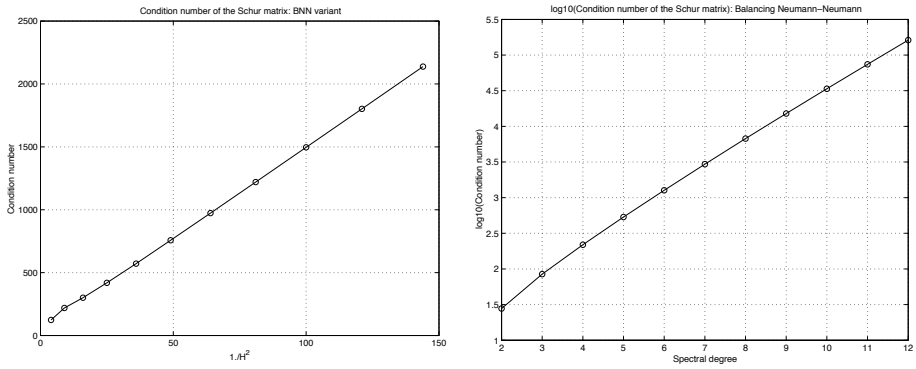

Figure 5: **Laplace problem on a boundary layer mesh**. Dependence of the condition number of the Schur matrix $\kappa(S_{NN})$ on the number of substructures (left) and dependence of the logarithm of the condition number of the Schur matrix $\kappa(S_{NN})$ on the spectral degree (right) (results from Tables 8 and 10).

7.4.2 Fixed partition

We now fix a macromesh $\mathcal{T}^{DD} = N_x \times N_y = 3 \times 3$ and investigate the dependence of the condition number on the spectral polynomial degree. The geometrically

Fixed spectral degree $k = 4$								
	No preconditioning				**NN**			
$N_x \times N_y$	It	λ_{max}	λ_{min}	$\kappa(S_{NN})$	It	λ_{max}	λ_{min}	$\kappa(P_{NN})$
2 x 2	28	32.708	0.26499	123.4328	9	2.3291	1	2.3291
3 x 3	71	43.421	0.19866	218.5623	12	2.8522	1	2.8522
4 x 4	105	43.422	0.1445	300.5059	15	2.9477	1	2.9477
5 x 5	132	43.422	0.10372	418.6499	17	2.9678	1	2.9678
6 x 6	149	43.423	0.075972	571.5622	19	2.978	1	2.978
7 x 7	164	43.423	0.057376	756.8057	20	2.9828	1	2.9828
8 x 8	179	43.423	0.044626	973.0352	20	2.986	1	2.986
9 x 9	194	43.423	0.035605	1219.5714	20	2.9881	1	2.9881
10 x 10	210	43.423	0.029025	1496.0529	21	2.9896	1	2.9896
11 x 11	226	43.423	0.024093	1802.2736	21	2.9908	1	2.9908
12 x 12	240	43.423	0.020309	2138.108	21	2.9916	1	2.9916

Table 8: **Laplace problem on a *boundary layer mesh* with** $\sigma_x = \sigma_y = 0.5$ **and** $n = 4$. Conjugate Gradient method for the Schur complement system without preconditioning and with Neumann-Neumann preconditioner: iteration counts, maximum and minimum eigenvalues, and condition number versus the number of subdomains.

refined grid $\mathcal{T}$ contains $(3+k) \times (3+k)$ elements; see Fig. 6 for the case $k = 6$.

Table 10 and Table 11 collect the results for the Balancing Neumann-Neumann and FETI preconditioners, respectively. Note the high condition numbers of unpreconditioned operators $\kappa(S_{NN})$ and $\kappa(F)$ for large k. Following (24) in section 6, we expect $\kappa(S_{NN})$ to grow as $k\,\sigma^{-(\beta\,k)}$, for a fixed partition. In Figure 5, right, $\log(\kappa(S_{NN}))$ is plotted versus the spectral degree. The results in Table 10 provide an estimated $\beta = 0.3014$, which is consistent with (24). On the other hand, as expected, $\kappa(P_{NN})$ and $\kappa(P_F)$ only grow as the square of the logarithm of the spectral degree; see Figure 7. This is in agreement with the bounds in (17) and (23). These results show that the condition numbers are independent of the aspect ratio of the mesh for this problem. Additional experiments (not presented here) on Problem IV on a geometric edge mesh with refinement only near one edge also lead to the same conclusion. We stress the fact that the original Schur complement has a condition number that grows *exponentially* with k, while our preconditioners provide a condition number that only grows *logarithmically* with k.

Fixed spectral degree $k = 4$								
	No preconditioning				**FETI**			
$N_x \times N_y$	It	λ_{max}	λ_{min}	$\kappa(F)$	It	λ_{max}	λ_{min}	$\kappa(P_F)$
2 x 2	47	17.68	0.13699	129.0591	10	2.9958	1.0011	2.9924
3 x 3	101	21.528	0.092123	233.6839	16	4.1547	1.0003	4.1536
4 x 4	123	23.334	0.092123	253.2879	21	3.9317	1.0005	3.9296
5 x 5	137	24.216	0.092123	262.8681	22	3.9216	1.0006	3.9191
6 x 6	148	24.691	0.092123	268.0171	23	3.9204	1.0006	3.9179
7 x 7	153	24.971	0.092123	271.0594	24	3.9202	1.0004	3.9185
8 x 8	158	25.149	0.092123	272.9957	24	3.9202	1.0006	3.9179
9 x 9	161	25.269	0.092123	274.3008	24	3.9202	1.0004	3.9187
10 x 10	163	25.354	0.092123	275.2208	24	3.9202	1.0005	3.9181
11 x 11	166	25.416	0.092123	275.8932	24	3.9202	1.0004	3.9187
12 x 12	168	25.463	0.092123	276.3992	24	3.9202	1.0005	3.9182

Table 9: **Laplace problem on a *boundary layer mesh* with $\sigma_x = \sigma_y = 0.5$ and $n = 4$.** Conjugate Gradient method for the FETI system without and with preconditioner: iteration counts, maximum and minimum eigenvalues, and condition numbers versus the number of subdomains.

7.5 Problem V: an interface problem

Singularities may sometimes occur not only in the neighborhood of boundaries of polygonal domains, as is investigated in Problem IV, but also at the interfaces of regions with different material properties. For example, interface problems in oil industry (cf. [45]) or electronic semiconductor device modeling (cf. [35]) may require highly refined meshes inside the computational domain. Such problems involving simultaneously jump coefficients and large aspect ratios of the mesh are extremely important in practice.

The interface problem is defined as in Problem II:

$$\begin{aligned} -\nabla \cdot (\rho \nabla u) &= 1, \quad \text{in } \Omega, \\ u &= u_D, \quad\quad \text{on } \partial\Omega. \end{aligned} \tag{30}$$

We assume that Ω is divided into four equal squares and that the coefficient ρ has a checkerboard distribution, given by $\rho_1 = 10^4$ and $\rho_2 = 1$. As domain decomposition partition $\mathcal{T}^{DD}$ we choose that given by ρ. We then have $N_x \times N_y = 2 \times 2$ substructures. In order to capture the interface effects, we have employed a geometrically refined mesh towards both sides of the interfaces $x = 1/2$ and $y = 1/2$. Since the purpose of this test case is to assess the properties of our preconditioners if anisotropic refinement takes place in the interior of Ω,

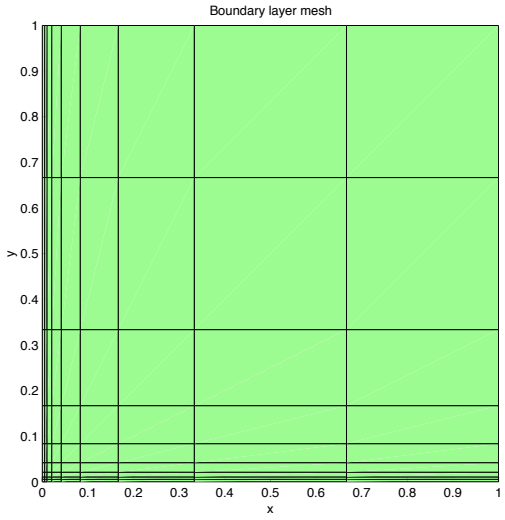

Figure 6: **Boundary layer mesh**. Refinement near two edges ($x = 0$ and $y = 0$) with 6 layers and mesh grading factors equal to $\sigma_x = 0.5$ and $\sigma_y = 0.5$. The unrefined grid is a fixed Cartesian grid of size $N_x \times N_y = 3 \times 3$.

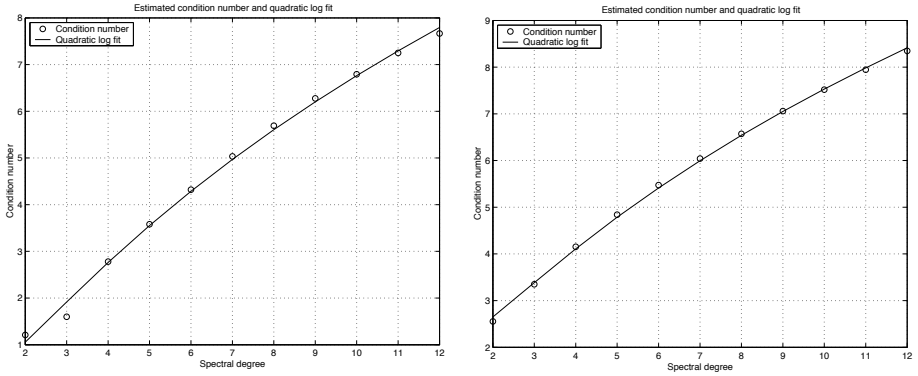

Balancing Neumann-Neumann FETI

Figure 7: **Laplace problem on a boundary layer mesh**. Estimated condition numbers (circles) and least-square second order logarithmic polynomial (solid line) versus the spectral degree for the Balancing Neumann-Neumann (left, results from Table 10) and the FETI (right, results from Table 11) preconditioned operators.

Fixed number of substructures $N_x \times N_y = 3 \times 3$								
	No preconditioning				**NN**			
k	It	λ_{max}	λ_{min}	$\kappa(S_{NN})$	It	λ_{max}	λ_{min}	$\kappa(P_{NN})$
2	18	13.09	0.47009	27.8466	8	1.2093	1	1.2093
3	39	23.584	0.27906	84.5135	10	1.5992	1	1.5991
4	71	43.421	0.19866	218.5623	12	2.7807	1	2.7806
5	118	82.489	0.15446	534.0585	13	3.5809	1.0001	3.5806
6	185	160.4	0.12649	1268.082	14	4.321	1.0001	4.3204
7	272	315.84	0.10716	2947.3406	15	5.034	1.0002	5.0331
8	344	625.76	0.092981	6729.9791	17	5.6913	1.0001	5.6906
9	424	1243.8	0.082121	15145.9124	17	6.2769	1.0001	6.2759
10	512	2476.8	0.073532	33683.7624	17	6.7937	1.0002	6.7924
11	608	4937.9	0.066568	74178.645	18	7.2527	1.0002	7.251
12	712	9852.1	0.060824	161978.5169	19	7.6679	1.0002	7.666

Table 10: **Laplace problem on a *boundary layer mesh* with** $\sigma_x = \sigma_y = 0.5$ **and** $n = k$. Conjugate Gradient method for the Schur complement system without preconditioning and with Balancing Neumann-Neumann preconditioner: iteration counts, maximum and minimum eigenvalues, and condition numbers versus the polynomial degree.

we have neglected the effects of the singularities at $\partial\Omega$. We are unaware of any theoretical study of this type of singularities. Figure 8 shows the refined mesh $\mathcal{T}$. As in Problem IV, the number of layers is determined only by the spectral polynomial degree k. Thus the highly refined mesh $\mathcal{T}$ consists of $(2 + 2k) \times (2 + 2k)$ quadrilaterals, thus providing an hp approximation of this problem. Mesh grading factors $\sigma_x = 0.75$ and $\sigma_y = 0.75$ have been considered in these numerical experiments.

The spectral polynomial degree k is varying from 2 to 8. Balancing Neumann-Neumann and one-level FETI preconditioners have been employed to solve Problem V; see Tables 12 and 13, respectively. The number of preconditioned Conjugate Gradient iterations seems to be bounded uniformly for growing k. The obtained results for the two preconditioners are not satisfactory. Figure 9 shows $\kappa(P_{NN})$ and $\kappa(P_F)$ versus the spectral degree k in a log-log plot: a linear behaviour is obtained, in contrast to all the other numerical experiments shown in this paper. Numerically $log(\kappa(P_{NN}))$ and $log(\kappa(P_F))$ are found to grow like k^p with $p = 0.8$ and $p = 0.74$, respectively. In section 6 we have provided a more pessimistic quadratic bound. We note the very small iteration counts obtained in this case, despite a linear growth in k.

Fixed number of substructures $N_x \times N_y = 3 \times 3$								
	No preconditioning				**FETI**			
k	It	λ_{max}	λ_{min}	$\kappa(F)$	It	λ_{max}	λ_{min}	$\kappa(P_F)$
2	40	11.092	0.3057	36.283	13	2.5551	1.0002	2.5545
3	69	16.1727	0.1696	95.3514	14	3.3502	1.0003	3.3490
4	101	21.5275	0.09212	233.6839	16	4.15468	1.00025	4.1536
5	157	27.0024	0.04849	556.8545	17	4.8423	1.0005	4.8399
6	214	32.4910	0.0249	1302.8742	18	5.4769	1.0006	5.4732
7	280	37.9728	0.01268	2994.9336	18	6.0492	1.0013	6.4125
8	352	43.4460	0.00649	6688.1144	19	6.5801	1.0012	6.5721
9	432	48.9158	0.0048	10140.5428	20	7.0699	1.0014	7.0597
10	520	54.38492	0.002428	22398.1226	20	7.5287	1.0013	7.5183
11	616	59.8554	0.0012	48165.1532	21	7.9582	1.0016	7.9449
12	720	65.3276	0.00065	99925.7334	20	8.3638	1.0018	8.3484

Table 11: **Laplace problem on a *boundary layer mesh* with** $\sigma_x = \sigma_y = 0.5$ **and** $n = k$. Conjugate Gradient method for the FETI system without and with preconditioner: iteration counts, maximum and minimum eigenvalues, and condition numbers versus the polynomial degree.

Fixed number of substructures $N_x \times N_y = 2 \times 2$								
	No preconditioning				**NN**			
k	It	λ_{max}	λ_{min}	$\kappa(S_{NN})$	It	λ_{max}	λ_{min}	$\kappa(P_{NN})$
2	19	26848	839.29	31.9891	4	2.1464	1	2.1464
3	34	27946	302.87	92.2692	6	2.9672	1	2.9672
4	47	28313	143.42	197.4121	6	3.7049	1	3.7049
5	60	28561	79.144	360.8691	6	4.4046	1	4.4046
6	73	28753	48.261	595.7833	6	5.0814	1	5.0814
7	85	28910	31.587	915.2486	7	5.7424	1	5.7424
8	98	29043	21.797	1332.4393	7	6.3915	1	6.3915

Table 12: **Interface problem**. Same legend as Table 10.

7.6 Problem VI: a reaction-diffusion problem

So far we have only considered purely diffusive problems. We now consider the following reaction-diffusion problem

$$\begin{aligned} -\varepsilon\,\nabla\cdot(\rho\,\nabla u) + u &= 1, \quad \text{in } \Omega, \\ u &= u_D, \quad \text{on } \partial\Omega. \end{aligned} \tag{31}$$

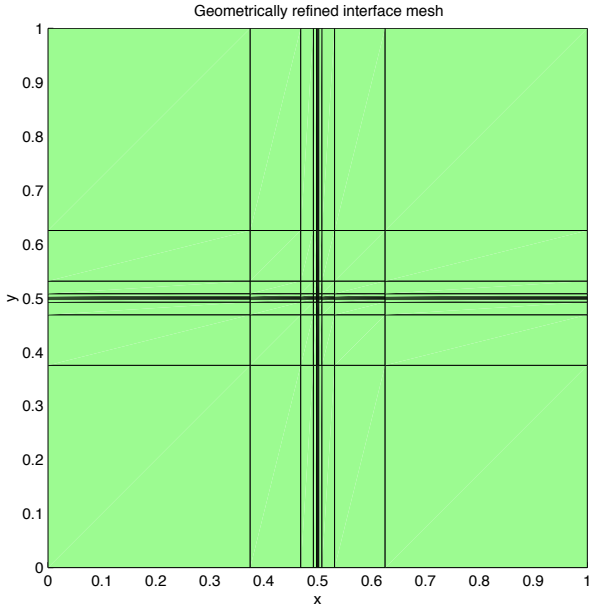

Figure 8: **Interface problem**. Anisotropic mesh with interior refinement for the case $n = k = 4$. Mesh grading factors $\sigma_x = 0.75$ and $\sigma_y = 0.75$.

Fixed number of substructures $N_x \times N_y = 2 \times 2$								
	No preconditioning				**FETI**			
k	It	λ_{max}	λ_{min}	$\kappa(F)$	It	λ_{max}	λ_{min}	$\kappa(P_F)$
2	24	18.903	0.00024261	7.7915E+04	4	2.8336	1	2.8335
3	34	41.593	0.00033396	1.2455E+05	4	3.6267	1	3.6265
4	40	79.826	0.00041491	1.9239E+05	4	4.3742	1.0001	4.3738
5	47	138.04	0.00049044	2.8147E+05	4	5.0978	1.0002	5.0971
6	50	220.55	0.00056243	3.9213E+05	4	5.8046	1.0002	5.8033
7	49	331.61	0.00063183	5.2485E+05	3	6.4982	1.0013	6.4899
8	48	475.52	0.00069917	6.8012E+05	3	7.1814	1.0015	7.171

Table 13: **Interface problem**. Same legend as Table 11.

The modified algorithm for the FETI method presented in section 5.3.4 has

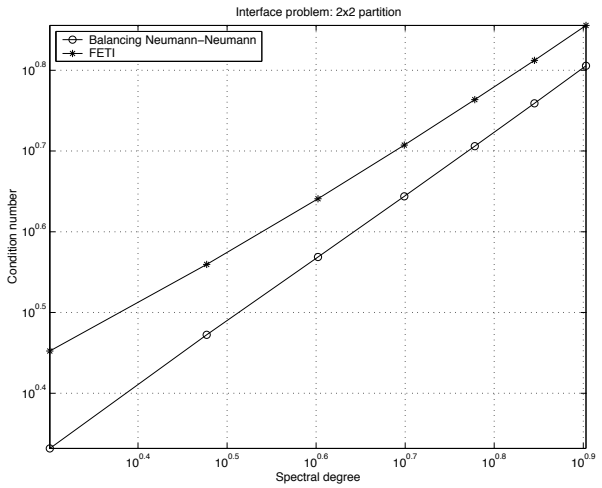

Figure 9: **Interface problem** . Condition numbers of the Balancing Neumann-Neumann (results from Table 12) and FETI (results from Table 13) preconditioners versus the spectral degree (log-log plot).

been adopted.

7.6.1 Reaction-diffusion problem on a boundary layer mesh

In this first part, we choose $(\varepsilon_x, \varepsilon_y) = (\varepsilon, \varepsilon), (\rho_x, \rho_y) = (1, 1), c = 1, f = 1$ in Problem (M)) with inhomogeneous Dirichlet boundary conditions. The source term is not compatible with the boundary conditions and thus boundary layers appear for ε small. Geometrically refined meshes are then needed in order to achieve exponential convergence and robustness with respect to ε; see, e.g., [30, 40]. Our main goal is here to analyse the convergence behaviour of Balancing Neumann-Neumann and one-level FETI preconditioners for different values of ε. In [44] some numerical experiments on the same problem were reported. Here however exact numerical integration is performed by using $GLL(k+1)$ nodes, while $GLL(k)$ nodes are employed in [44]. We note that the analysis provided in [44] does not cover the case of reaction-diffusion problems.

Since boundary layer effects are present, the size of the thinnest layer $H\sigma^k$ should be comparable to the size of the boundary layer $\sqrt{\varepsilon}$; see [30, 40]. In addition, singularity resolution requires that n be comparable to k. These assumptions lead to the following relation to determine the level of refinement n

and the spectral polynomial degree k when $\varepsilon < 1$:

$$n = n(\varepsilon) = \left[\frac{\log(\sqrt{\varepsilon}/H)}{\log \sigma}\right] + 1, \quad k = k(\varepsilon) = n(\varepsilon),$$

where $[x]$ denotes the integer part of x. For $\varepsilon = 1$, no refinement is performed ($n = 0$) and the spectral polynomial degree k is fixed to 2. The macromesh $\mathcal{T}^{DD}$ consists of 5×5 substructures ($H = 1/5$). Geometric refinement is performed towards the two intersecting edges $x = 0$ and $y = 0$ only, with mesh grading factors $\sigma = \sigma_x = \sigma_y = 0.5$ as in Problem IV. The refined grid $\mathcal{T}$ contains thus $(5 + k) \times (5 + k)$ elements. We stress the fact that ε determines both n and k, and that we have here a genuinely *hp* approximation.

Fixed number of substructures $N_x \times N_y = 5 \times 5$								
	No preconditioning				**NN**			
ε	It	λ_{max}	λ_{min}	$\kappa(S_{NN})$	It	λ_{max}	λ_{min}	$\kappa(P_{NN})$
1	26	5.2014	2.6711E-01	19.473	8	1.1283	1	1.1283
10^{-1}	26	5.2365E-01	3.7749E-02	13.872	8	1.118	1	1.118
10^{-2}	38	1.2148E-01	8.7128E-03	13.943	9	1.201	1	1.201
10^{-3}	46	2.2411E-02	8.8427E-04	25.344	7	1.1215	1	1.1214
10^{-4}	96	7.9440E-03	5.1737E-05	153.55	6	1.0962	1.	1.0962
10^{-5}	98	1.5527E-03	7.4854E-06	207.42	5	1.0668	1	1.0668
10^{-6}	156	6.0903E-04	8.5442E-07	712.80	5	1.079	1	1.079
10^{-7}	226	2.4205E-04	1.2950E-07	1869.1	4	1.0724	1	1.0724
10^{-8}	278	8.0628E-05	3.5222E-08	2289.2	4	1.0686	1	1.0686

Table 14: **Reaction-diffusion problem on a boundary layer mesh**. Same legend as Table 6.

Table 14 and Table 15 show the results for both preconditioners. We note that for $\varepsilon = 0$ the stiffness matrix A reduces to the mass matrix but mass matrices arising from spectral elements are not necessarily uniformly well-conditioned with respect to k even for shape-regular meshes. For one single spectral element, their condition number is expected to grow as k^2; see [44]. Both Balancing Neumann-Neumann or FETI preconditioners lead to very satisfactory results and the convergence behaviour is thus robust with respect to ε as well. In [44], fewer preconditioned CG iterations were found for ε very small. There however integrals were calculated using a lower precision quadrature formula and diagonal mass matrices were obtained, which might explain this difference.

Fixed number of substructures $N_x \times N_y = 5 \times 5$								
	No preconditioning				**FETI**			
ε	It	λ_{max}	λ_{min}	$\kappa(F)$	It	λ_{max}	λ_{min}	$\kappa(P_F)$
1	90	369.71	0.715	517.0762	14	1.7019	1.0005	1.7011
10^{-1}	65	387.73	7.1105	54.5294	13	1.5924	1.0005	1.5916
10^{-2}	59	776.62	34.002	22.8405	12	1.4339	1.0008	1.4328
10^{-3}	67	5303.3	182.53	29.0546	10	1.149	1.0003	1.1486
10^{-4}	135	77900.27	509.25	152.9706	9	1.0987	1.0005	1.0981
10^{-5}	144	556787.37	2598.3	214.2891	8	1.0742	1.001	1.0731
10^{-6}	234	5091439.9	6603.1	771.0798	9	1.0858	1.0011	1.0845
10^{-7}	355	34374460	16586.1	2072.4985	8	1.0802	1.0009	1.0793
10^{-8}	453	127239000	49764	2556.85	8	1.0766	1.0007	1.0758

Table 15: **Reaction-diffusion problem on a boundary layer mesh**. Same legend as Table 7.

7.6.2 Reaction-diffusion problem with variable coefficient jumps

In this part, we investigate a reaction-diffusion problem with variable coefficient jumps corresponding to the choice $(\varepsilon_x, \varepsilon_y) = (1, 1), (\rho_x, \rho_y) = (\rho, \rho), c = 1, f = 1$ in Problem (M), with inhomogeneous Dirichlet boundary conditions. Since ε is fixed, the same uniform meshes as in section 7.2.2 are employed. In particular, we consider two partitions with $N_x \times N_y = 3 \times 3$ and $N_x \times N_y = 5 \times 5$ and a checkerboard distribution for ρ as in the test cases in section 7.2. The spectral polynomial degree is fixed to 10. In addition, $\rho_1 = 1$ is fixed, whereas ρ_2 is varying from 1 to 10^6. Since unrefined meshes are used, $\mathcal{T}^{DD}$ and $\mathcal{T}$ coincide here.

The results are presented in Table 16 for both partitions and preconditioners. In section 7.2.2, the $GLL(k)$ basis has been chosen for numerical integration. As already stated, this basis leads to exact numerical integration for purely diffusive problems with piecewise constant coefficients. In order to allow a comparison with Table 5, this basis has also been used here, although it does not lead to exact integration for Problem VI due to the presence of the reaction term. The same behaviour as in section 7.2.2 (see Table 5) is observed. For growing ρ_2, the iteration count It decreases, whereas the condition number of the preconditioned operators is bounded independently of the ratio ρ_2/ρ_1. Our preconditioners are thus found to be robust with respect to the jump of the coefficients also for reaction-diffusion problems.

Fixed number of substructures $N_x \times N_y = 3 \times 3$								
	NN				**FETI**			
ρ_2	It	λ_{max}	λ_{min}	$\kappa(P_{NN})$	It	λ_{max}	λ_{min}	$\kappa(P_F)$
1	14	3.6148	1	3.6148	14	6.1865	1.0011	6.1798
10	14	2.8565	1	2.8565	12	4.2766	1.0004	4.2747
10^2	11	2.5369	0.99389	2.5525	9	3.2335	1.0003	3.2324
10^3	8	2.4877	1	2.4877	8	3.1097	1.0001	3.1094
10^4	7	2.4825	1	2.4825	7	3.0972	1	3.0971
10^5	6	2.482	1	2.482	6	3.0959	1	3.0959
10^6	7	2.482	1	2.482	5	3.0958	1	3.0958
Fixed number of substructures $N_x \times N_y = 5 \times 5$								
	NN				**FETI**			
ρ_2	It	λ_{max}	λ_{min}	$\kappa(P_{NN})$	It	λ_{max}	λ_{min}	$\kappa(P_F)$
1	24	3.7605	1	3.7605	22	5.64	1.0009	5.6348
10	19	2.9473	1	2.9472	20	3.9267	1.0008	3.9236
10^2	14	2.5197	1	2.5197	15	3.0278	1.0004	3.0264
10^3	12	2.4671	1	2.4671	12	2.9214	1.0002	2.9209
10^4	11	2.4616	0.99714	2.4687	11	2.9106	1	2.9106
10^5	10	2.4611	0.99998	2.4611	11	2.9095	1	2.9095
10^6	10	2.461	0.99992	2.4612	10	2.9094	1	2.9094

Table 16: **Reaction-diffusion problem with variable coefficient jumps. Case of** $k = 10$ **and** $\rho_1 = 1$. Conjugate Gradient method for the Balancing Neumann-Neumann and FETI preconditioned operators: iteration counts, maximum and minimum eigenvalues, and condition numbers versus ρ_2.

8 Perspectives

Many important issues remain to be partially or fully addressed:
We have only considered exact solvers for systems involving local Schur complements or their inverses. Approximate local solvers (see, e.g., [21]) are often needed for very large problems. This aspect is especially important for three-dimensional applications in order to reduce the computational cost of this step.

As already stated, a crucial issue to be addressed is the treatment of hanging nodes in our framework. This would allow to treat specific problems that may mix difficulties (corner singularities, boundary layer effects) defined on more complicated domains. In our numerical experiments, we have shown that

boundary layer meshes can handle such situations. Nevertheless mesh including hanging nodes are better suited when only singularities are present, since they involve fewer degrees of freedom and thus give smaller algebraic linear systems to solve; see the remarks at the end of section 4. We believe that the analysis and the development of iterative substructuring methods for general meshes with hanging nodes still need to be fully addressed. The algorithms in [31] for instance can be certainly be employed when hanging nodes are present on the interface Γ and the analysis proposed in [44] can be carried out using stable extensions for meshes with hanging nodes (see, e.g., [38, Sect. 4.6.3]). However there is not a straightforward way of defining a Neumann-Neumann or a FETI algorithm in this case; see Remark 6.1 in [44].

We have only considered scalar elliptic problems. The generalization of our preconditioners to advection-diffusion problems (see Remark 2.1) or to saddle-point problems on geometrically refined meshes remains open.

Finally the development and analysis of Neumann-Neumann and FETI methods for three dimensional approximations on geometrically refined meshes also remain open problems.

References

[1] Yves Achdou, Patrick Le Tallec, Frédéric Nataf, and Marina Vidrascu. A domain decomposition preconditioner for an advection-diffusion problem. *Comput. Methods Appl Mech. Engrg.*, 184:145–170, 2000.

[2] Mark Ainsworth. A preconditioner based on domain decomposition for *hp*–FE approximation on quasi–uniform meshes. *SIAM J. Numer. Anal.*, 33:1358–1376, 1996.

[3] Borje Andersson, U. Falk, Ivo Babuška, and Tobias von Petersdorff. Reliable stress and fracture mechanics analysis of complex aircraft components using a *hp*–version FEM. *Int. J. Numer. Meth. Eng.*, 38(13):2135–2163, 1995.

[4] Ivo Babuška, Alan Craig, Jan Mandel, and Juhani Pitkäranta. Efficient preconditioning for the p-version finite element method in two dimensions. *SIAM J. Numer. Anal.*, 28(3):624–661, 1991.

[5] Ivo Babuška and Benqi Guo. Approximation properties of the *hp*–version of the finite element method. *Comp. Methods Appl. Mech. Eng.*, 133:319–346, 1996.

[6] Zhaojun Bai, James Demmel, Jack Dongarra, Axel Ruhe, and Henk Van der Vorst. *Templates for the Solution of Algebraic Eigenvalue Problems: A Practical Guide*. SIAM, Philadelphia, PA, 2000.

[7] Richard Barrett, Michael Berry, Tony F. Chan, James Demmel, June Donato, Jack Dongarra, Victor Eijkhout, Roldan Pozo, Charles Romine, and Henk Van der Vorst. *Templates for the Solution of Linear Systems: Building Blocks for Iterative Methods, 2nd Edition*. SIAM, Philadelphia, PA, 1994.

[8] Christine Bernardi and Yvon Maday. Spectral methods. In *Handbook of Numerical Analysis, Vol. V, Part 2*, pages 209–485. North-Holland, Amsterdam, 1997.

[9] Ion Bica. *Iterative substructuring algorithms for the p–version finite element method for elliptic problems*. PhD thesis, Courant Institute, New York University, 1997.

[10] Susanne C. Brenner. The condition number of the Schur complement in domain decomposition. *Numer. Math.*, 83:187–203, 1999.

[11] Maksymilian Dryja, Marcus V. Sarkis, and Olof B. Widlund. Multilevel Schwarz methods for elliptic problems with discontinuous coefficients in three dimensions. *Numer. Math.*, 72(3):313–348, 1996.

[12] Maksymilian Dryja and Olof B. Widlund. Schwarz methods of Neumann-Neumann type for three-dimensional elliptic finite element problems. *Comm. Pure Appl. Math.*, 48(2):121–155, February 1995.

[13] Charbel Farhat and Po-Shu Chen. A scalable Lagrange multiplier based domain decomposition method for time-dependent problems. *Int. J. Numer. Meth. Engng.*, 38:3831–3853, 1995.

[14] Charbel Farhat, Michel Lesoinne, Patrick LeTallec, Kendall Pierson, and Daniel Rixen. FETI-DP: a dual-primal unified FETI method. I. A faster alternative to the two-level FETI method. *Internat. J. Numer. Methods Engrg.*, 50(7):1523–1544, 2001.

[15] Charbel Farhat and François-Xavier Roux. Implicit parallel processing in structural mechanics. In J. Tinsley Oden, editor, *Computational Mechanics Advances*, volume 2 (1), pages 1–124. North-Holland, 1994.

[16] Charbel Farhat and Francois-Xavier Roux. A method of finite element tearing and interconnecting and its parallel solution algorithm. *Int. J. Numer. Meth. Engng.*, 32:1205–1227, 1991.

[17] Gene Golub and Charles Van Loan. *Matrix Computations*. The John Hopkins University Press, 1996. Third edition.

[18] Benqi Guo and Weiming Cao. A preconditioner for the *hp*–version of the finite element method in two dimensions. *Numer. Math.*, 75:59–77, 1996.

[19] Benqi Guo and Weiming Cao. Additive Schwarz methods for the *hp* version of the finite element method in two dimensions. *SIAM Journal on Scientific Computing*, 18(5):1267–1288, 1997.

[20] Benqi Guo and Weiming Cao. An additive Schwarz method for the *hp*–version of the finite element method in three dimensions. *SIAM J. Numer. Anal.*, 35:632–654, 1998.

[21] Axel Klawonn and Olof B. Widlund. A domain decomposition method with Lagrange multipliers and inexact solvers for linear elasticity. *SIAM J. Sci. Comput.*, 22(4):1199–1219, October 2000.

[22] Axel Klawonn and Olof B. Widlund. FETI and Neumann-Neumann iterative substructuring methods: connections and new results. *Comm. Pure Appl. Math.*, 54(1):57–90, 2001.

[23] Axel Klawonn, Olof B. Widlund, and Maksymilian Dryja. Dual-Primal FETI methods for three-dimensional elliptic problems with heterogeneous coefficients. Technical Report 815, Department of Computer Science, Courant Institute, April 2001.

[24] Jan Mandel. Iterative methods for p–version finite elements: preconditioning thin solids. *Comp. Methods Appl. Mech. Eng.*, 133:247–257, 1996.

[25] Jan Mandel and Marian Brezina. Balancing domain decomposition for problems with large jumps in coefficients. *Math. Comp.*, 65:1387–1401, 1996.

[26] Jan Mandel and G. Scott Lett. Domain decomposition preconditioning for p–version finite elements with high aspect ratios. *Appl. Num. Math.*, 8:411–425, 1991.

[27] Jan Mandel and Radek Tezaur. Convergence of a substructuring method with Lagrange multipliers. *Numer. Math.*, 73:473–487, 1996.

[28] Jan Mandel and Radek Tezaur. On the convergence of a dual-primal substructuring method. *Numer. Math.*, 88(3):543–558, January 2001.

[29] Jens Markus Melenk. On condition numbers in *hp*-FEM with Gauss-Lobatto-based shape functions. *J. Comput. Appl. Math.*, 139(1):21–48, 2002.

[30] Jens Markus Melenk and Christoph Schwab. *hp*–FEM for reaction–diffusion equations. I: Robust exponential convergence. *SIAM J. Numer. Anal.*, 35:1520–1557, 1998.

[31] John Tinsley Oden, Abani Patra, and Yusheng Feng. Parallel domain decomposition solver for adaptive *hp* finite element methods. *SIAM J. Numer. Anal.*, 34:2090–2118, 1997.

[32] Luca F. Pavarino. Neumann-Neumann algorithms for spectral elements in three dimensions. *RAIRO Mathematical Modelling and Numerical Analysis*, 31:471–493, 1997.

[33] Luca F. Pavarino and Olof B. Widlund. Balancing Neumann-Neumann algorithms for incompressible Navier-Stokes equations. *Commun. Pure Appl. Math.*, 55:302–335, 2002.

[34] Joaquim Peiró, Sergio Giordana, C. Griffith, and Spencer Sherwin. High-order algorithms for vascular flow modelling. *Int. J. Num. Meth. Fluids*, 40(1-2):137–151, 2002.

[35] S.J. Polak, C. Den Heijer, W.H. Schilders, and P. Markowich. Semiconductor device modelling from the numerical point of view. *Int. J. for Num. Methods in Eng.*, 24:763–838, 1987.

[36] Alfio Quarteroni and Alberto Valli. *Numerical Approximation of Partial Differential Equations*. Springer-Verlag, Berlin, 1994.

[37] Marcus V. Sarkis. *Schwarz Preconditioners for Elliptic Problems with Discontinuous Coefficients Using Conforming and Non-Conforming Elements*. PhD thesis, Courant Institute, New York University, September 1994. TR671, Department of Computer Science, New York University, `URL: file://cs.nyu.edu/pub/tech-reports/tr671.ps.Z`.

[38] Christoph Schwab. *p– and hp– Finite Element Methods*. Oxford Science Publications, 1998.

[39] Christoph Schwab and Manil Suri. The p and hp version of the finite element method for problems with boundary layers. *Math. Comp.*, 65:1403–1429, 1996.

[40] Christoph Schwab, Manil Suri, and Christos A. Xenophontos. The hp–FEM for problems in mechanics with boundary layers. *Comp. Methods Appl. Mech. Eng.*, 157:311–333, 1998.

[41] Barry F. Smith, Petter E. Bjørstad, and William D. Gropp. *Domain Decomposition: Parallel Multilevel Methods for Elliptic Partial Differential Equations*. Cambridge University Press, 1996.

[42] Clemens-August Thole and Klaus Stüben. Industrial simulation on parallel computers. *Parallel Computing*, 25:2015–2037, 1999.

[43] Andrea Toselli. FETI domain decomposition methods for scalar advection-diffusion problems. *Comp. Methods Appl. Mech. Eng.*, 190:5759–5776, 2001.

[44] Andrea Toselli and Xavier Vasseur. Domain decomposition methods of Neumann-Neumann type for hp-approximations on geometrically refined boundary layer meshes in two dimensions. Technical Report 02–15, Seminar für Angewandte Mathematik, ETH, Zürich, September 2002. Submitted to Numerische Mathematik.

[45] C. Vuik, A. Segal, and J.A. Meijerink. An efficient preconditioned CG method for the solution of a class of layered problems with extreme contrasts in the coefficients. *J. Comput. Phys.*, 152:385–403, 1999.

Research Reports

No.	Authors	Title
02-20	A. Toselli, X. Vasseur	A numerical study on Neumann-Neumann and FETI methods for *hp*-approximations on geometrically refined boundary layer meshes in two dimensions
02-19	D. Schötzau, Th.P. Wihler	Exponential convergence of mixed *hp*-DGFEM for Stokes flow in polygons
02-18	P.-A. Nitsche	Sparse approximation of singularity functions
02-17	S.H. Christiansen	Uniformly stable preconditioned mixed boundary element method for low-frequency electromagnetic scattering
02-16	S.H. Christiansen	Mixed boundary element method for eddy current problems
02-15	A. Toselli, X. Vasseur	Neumann-Neumann and FETI preconditioners for *hp*-approximations on geometrically refined boundary layer meshes in two dimensions
02-14	Th.P. Wihler	Locking-Free DGFEM for Elasticity Problems in Polygons
02-13	S. Beuchler, R. Schneider, C. Schwab	Multiresolution weighted norm equivalences and applications
02-12	M. Kruzik, A. Prohl	Macroscopic modeling of magnetic hysteresis
02-11	A.-M. Matache, C. Schwab, T. von Petersdorff	Fast deterministic pricing of options on Lévy driven assets
02-10	D. Schötzau, C. Schwab, A. Toselli	Mixed *hp*-DGFEM for incompressible flows
02-09	Ph. Frauenfelder, Ch. Lage	Concepts - An object-oriented software package for partial differential equations
02-08	A.-M. Matache, J.M. Melenk	Two-Scale Regularity for Homogenization Problems with Non-Smooth Fine Scale Geometry
02-07	G. Schmidlin, C. Lage, C. Schwab	Rapid solution of first kind boundary integral equations in $\mathbb{R}^3$
02-06	M. Torrilhon	Exact Solver and Uniqueness Conditions for Riemann Problems of Ideal Magnetohydrodynamics
02-05	C. Schwab, R.-A. Todor	Sparse Finite Elements for Elliptic Problems with Stochastic Data
02-04	R. Jeltsch, K. Nipp	CSE Program at ETH Zurich: Are we doing the right thing?